2009

Particle size characterization of ultrasonic treatment of dry milling coproducts for enhanced biofuel production

Cody John Hearn
Iowa State University

Particle size characterization of ultrasonic treatment of dry milling coproducts for enhanced biofuel production

by:

Cody John Hearn

A thesis submitted to the graduate faculty

in partial fulfillment of the requirements for the degree of:

MASTER OF SCIENCE

Major: Industrial & Agricultural Technology

Program of Study Committee:
David Grewell, Major Professor
Robert T. Burns
John K. Jackman

Iowa State University

Ames, Iowa

2009

This paper is dedicated to my loving parents, family, and friends.

TABLE OF CONTENTS

LIST OF FIGURES

LIST OF FIGURES (continued)

LIST OF TABLES

ACKNOWLEDGMENTS

I want to give special thanks to Dr. David Grewell for his guidance and support.

I also want to give thanks to everyone that has helped me along the way.

ABSTRACT

This study characterized the use of ultrasonic energy to increase the production of the methane as a biogas from the anaerobic digestion of coproducts of dry milling. Dried distillers grain with solubles (DDGs), solids, thin stillage, and corn syrup were treated with various ultrasonic conditions and compared to untreated (control) samples. The amplitude ranged from 52.8 μm_{pp} to 160 μm_{pp} and the time was varied from 10 to 50 s. The resulting samples were characterized using scanning electron and optical microscopy (SEM, OM) and particle size analysis. Samples consisting of solid/liquid suspensions (DDGs, solids) showed a significant decrease in particle size (44.5% decrease in DDGS and 42.9% decrease in solids) and an associated increase in the surface area to volume ratio, thus promoting anaerobic digestion for enhanced biochemical methane production (BMP). In addition, thin stillage and corn syrup exhibited a slight increase in the peak particle size. It should be noted that the overall mean particle size decreased (65.73% decrease in syrup, and 74.57% in thin stillage) despite that the peak particle size increased. This observation is counter intuitive to ultrasonic treatment and is believed to be the result of oil agglomeration after being released from lipid bio-layers.

CHAPTER 1: INTRODUCTION

1.0 Vision

As industrialized nations search for alternative fuels to supply the growing need for more energy sources, research in bio-fuels has increased. The vision of this research is to improve biogas production by various ultrasonic treatments (amplitude and time) of selected dry mill ethanol production co-products and promoting anaerobic digestion for enhanced biochemical methane production (BMP).

1.1 Origin of corn

Mesoamerica extends from northern Mexico to Central America as seen in Figure 1.1. The region's environmental diversity, from arid landscapes and mountainous areas to tropical lowlands, played a large role in the area becoming the source of ancestral forms of major present-day crops, including corn [1]. Native Americans grew maize (more commonly called corn) at least 5600 years ago. Scientists and historians believe the Mesoamerican natives first tamed wild relatives of corn to turn them into a usable food crops. To make it edible, the corn was typically ground into flour or soaked in lye or other substances to soften the outer shell [2]. Although there have been many theories, the precise origin of corn remains uncertain, as the plant is found only in cultivation and does not grow in the wild [3].

Figure 1.1 Mesoamerica [4]

1.2 Types of corn

There are five main types of corn: dent corn, flint corn, sweet corn, waxy corn, and popcorn. Figure 1.2 shows some of these varieties. Dent corn *(Zea mays indenata)*, commonly referred to as field corn, and is often used as livestock feed, in industrial products or in processed foods. Either white or yellow, dent kernels contain both hard and soft starches that become indented as the crop matures. [5]

Figure 1.2 Corn types [6]

Flint corn *(Zea mays indurate),* popularly known as Indian corn, is often used for purposes similar to those for dent corn. Flint corn is distinguished from other corn varieties with kernels having a range of colors from white to red. Today, most flint corn is grown in Central and South America [5].

Sweet corn *(Zea saccharata* or *Zea rugosa)* can be eaten from the cob, or it can be canned or frozen for future consumption. Sweet corn is seldom used for feed or flour and has a softer outer shell because it is harvested before the kernel matures and hardens. Sweet corn is typically sweeter in taste than dent and flint corn because it contains more natural sugars [5].

Waxy corn, discovered in the early 1900's in China, is very similar to dent corn, but it has its own distinctive characteristic: it is composed entirely of amylopectin (a starch

composed of branched glucose chains); while dent corn contains 75% amylopectin and 25 percent amylase (composed of unbranched glucose chains). Research is currently being done at many universities to exploit its unique traits [7].

Popcorn is unique in that it is not initially edible like sweet corn. Kernels are cooked, usually in oil or in the presence of a heat source alone, until the insides of the kernels explode through the tough outer shells. Its origins date back over 1000 years to Native Americans, who introduced it to early settlers and explorers [8].

Dent corn, the type used in this study, is higher in starch and lower in sugar than sweet corn. The stalks of dent corn typically grow taller than those of the sweet corn, and their individual kernels have distinctive dentations on their sides, probably leading to the common name. The corn itself is often dried for processing and is obtainable in a number of different forms including whole cobs, individual kernels, and ground flours. Dent corn grows best in regions with long summers that allow the ears of corn to fully mature, and when cultivated appropriately dent corn usually can be stored for around two years [9].

Dent corn is also one of the most cultivated crops worldwide and has a wide range of uses. Dent corn is commonly found in animal feeds; since it is inexpensive to grow, it is often used as a bulk additive for improved livestock supplementation [9]. In addition to being a source of food for humans and livestock, dent corn contains starch and other coproducts that can be processed into many other useful items, including biodegradable plastics, alcohols, cosmetic and skin care products, drugs, batteries, rubber, beverages, crayons, soaps,

absorbent materials for diapers, food additives, food supplements, and other commercial products [10]. Because dent kernel corn has a variety of uses, it is very important economically in some regions of the United States [9].

1.3 Properties of the corn kernel

A kernel of corn is wrapped in a hard fibrous outer shell. Inside the kernel is the germ, or embryo, from which a new corn plant can develop. These parts of the kernel can be seen in Figure 1.3. Around the germ is the kernel's food supply, the endosperm, which is mostly starch. When the kernel germinates, it draws nourishment from the endosperm until it develops roots and obtains nutrients from the soil. The endosperm of the kernel accounts for approximately 82% of the kernel's dry weight. The starch is the most extensively used potion of the kernel. Starch is used in foods or as a key component in biofuels, sweeteners, and bioplastics, and other products [11].

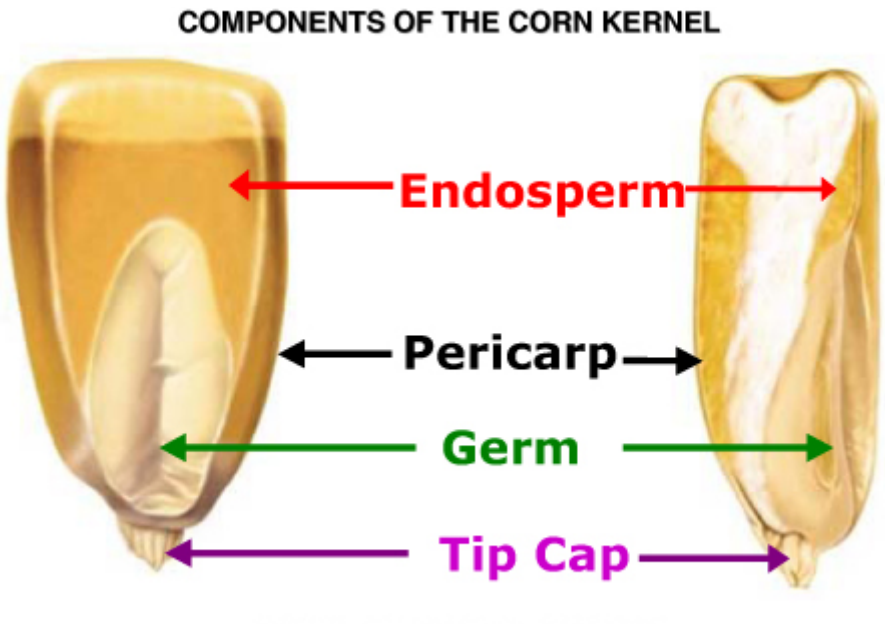

Figure 1.3 Corn kernel [13]

The pericarp is the hard fibrous outer covering that protects the kernel and preserves the nutrient value of the endosperm inside. The pericarp resists water, many insects and microorganisms.

The germ is the only living part of the corn kernel itself after the corn has fully matured. The germ contains the vital genetic sequence, enzymes, vitamins, and minerals required for the kernel to grow into a fully developed corn plant. Roughly 25% of the germ consists of corn oil (typically high in polyunsaturated fats.) The “tip cap” connects the kernel to the cob. Water and nutrients flow into the kernel through the tip cap, and it is the only portion of the kernel that is not covered by the pericarp [12].

1.4 Components and uses of corn

Each corn kernel contains four main chemistries: starch, protein, oil, and fiber. These components are processed to create a wide range of products [14].

Figure 1.4 Corn products [15]

For example, there are numerous food, drug, cosmetic, and industrial applications for cornstarch. A few of these examples can be seen in Figure 1.4. The starch is also often converted into dextrose (a pure crystalline sugar) or corn syrup, which also have multiple consumer and industrial uses. Products and processes that use cornstarch include batteries, bookbinding, papers, fireworks, lubricants, paints, oil refining, baby food, mustard, beer and ale, chewing gum, sauces and gravies, antibiotics, lipstick, lotions, soaps, and pet foods. Dextrose is used in food (e.g., carbonated beverages, chocolate, peanut butter, yeast, wine, condensed milk, and doughnuts, among others) and in many pharmaceutical and industrial applications, including leather tanning, rubber, adhesives, biodegradable plastics, textiles, electroplating and galvanizing, coatings for pills, medicinal syrups, and even intravenous

injections. Dried or aqueous corn syrups also are used in many industrial and medical products. These include shoe polish, rayon, theatrical makeup, plasticizing agents, fermentation processes, cereals, desserts, canned fruits and vegetables, maple syrup, marshmallows, frozen and dried eggs, and an assortment of snack foods [14].

The solubles from a milling process also provide a significant feedstock for various products. For example the steep water is useful in the production of antibiotics, chemicals, pharmaceuticals, and yeast. Some examples of solubles uses are: paints, varnishes, insecticides, rubber substitutes, livestock feed, rust preventative, margarine, mayonnaise, cooking oil, salad dressings, vitamins, antibiotics, and soap [14].

Another common coproduct from milling corn is corn gluten. Gluten meal is protein rich and is used primarily in animal feed for poultry and swine, and in pet food. The fiber in corn, much of which comes from the hull of the corn, is made into a feed product called gluten feed. It is used mostly in beef and dairy cattle provisions. The germ can also be ground into meal for animal feed. Approximately 25% of the germ is corn oil, which has food, drug, and manufacturing uses [16].

1.5 U.S. corn production

Corn is the most widely produced feed grain in the United States, accounting for 90% of the total grains. It is estimated that 80 million acres of land are planted with corn every year [17]. Furthermore, the United States is the largest corn producer in the world. In 2003, corn growers in the United States produced 256.9 million metric tons (MMT) of corn, exporting nearly 20% of the crop (51.0 MMT). The top five destinations for U.S. corn are Japan, Mexico, Taiwan, Canada, and Egypt as shown in Figure 1.5. [18].

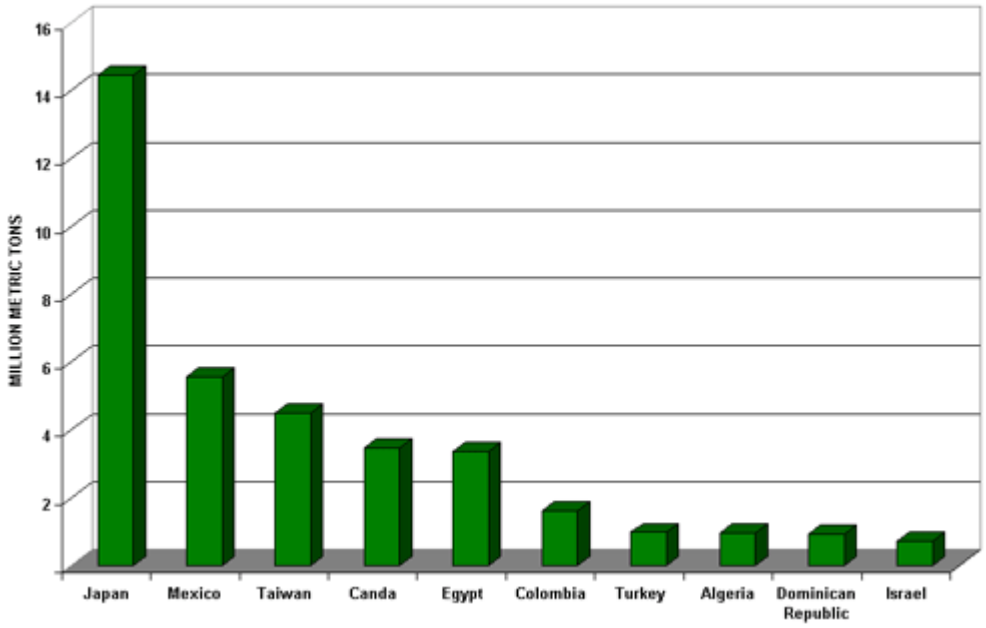

Figure 1.5 Top 2003 U.S. corn customers [18]

1.6 U.S. production of corn-based ethanol

The production of corn-based ethanol in the United States is dramatically increasing, due primarily to the increased demand for ethanol as a fuel additive. According to the Renewable Fuels Association (RFA), in 2007 the United States had 134 ethanol plants operational and 77 plants being built. A map of the plant locations is shown in figure 1.7. Production has increased by a factor of 27 since 1980 [19]. As corn-based ethanol production is increasing, there is a corresponding increase in coproducts.

Coproducts from ethanol production are primarily used as livestock feeds, which can provide ethanol producers with a significant secondary revenue source and increase the profitability of the ethanol production process. With increasing numbers of ethanol plants, the industry is finding new applications for the resulting coproducts in order to increase the economic viability of ethanol. Coproducts such as distillers grains (see Figure 1.6) with solubles (DDGS), solids, syrups, and thin stillage have potential for value-added processing [20]. While many of these coproducts are currently used as animal feed, they also have the potential to produce methane gas through anaerobic digestion [21].

Figure 1.6 DDGS pile [22]

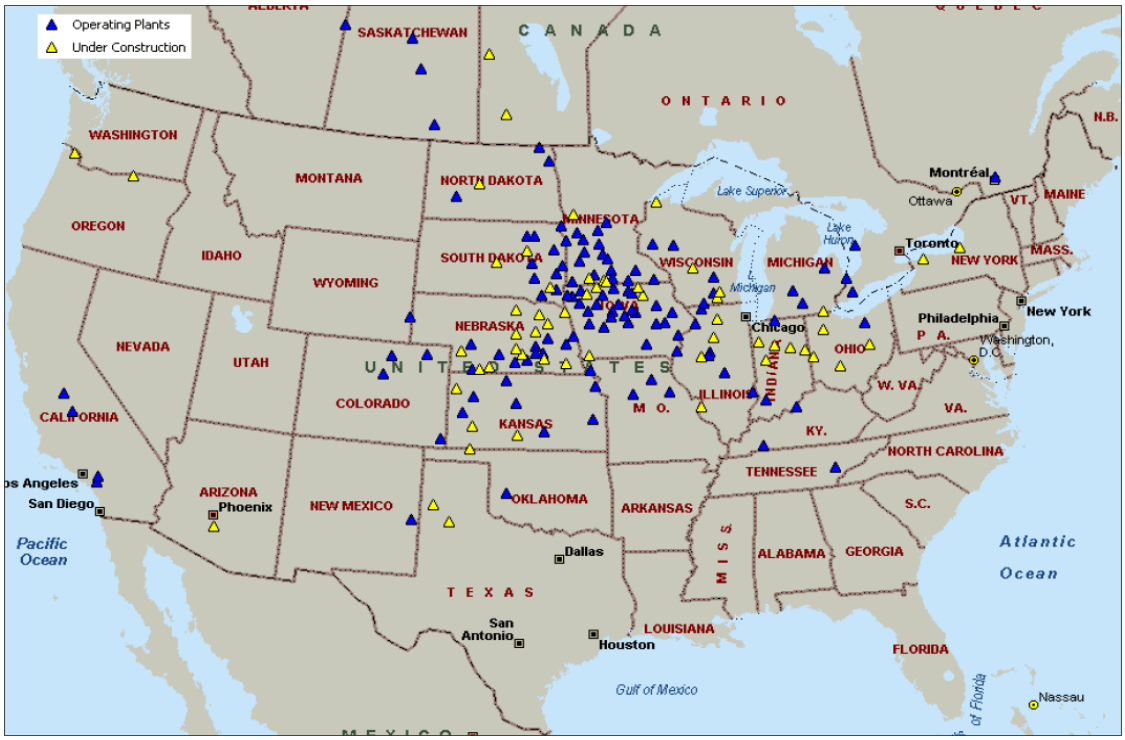

Figure 1.7 U.S. ethanol facilities [23]

Ethanol can be produced from corn by either wet milling or dry grind processing. In wet milling the corn kernel is separated into different components, which results in a number of products.

In dry grind facilities the corn kernel components are not separated, and the main coproduct is distillers dried grains with solubles (DDGS). Dry grind plants typically require less equipment and capital compared to wet mills plants. The vast majority of the increase in ethanol production during the past decade is credited to growth in the dry grind industry. The sale of the coproducts produced at ethanol plants provides an additional revenue source [24].

There have been many studies in recent years to estimate the energy used to produce ethanol. The studies have resulted in a wide range of estimates due to the variation in the source of data collected and assumptions built into the models. A recent study in 1995 by H. Shapouri, J. Duffield, and M. Graboski for the U.S. Department of Agriculture showed that the net energy value of corn ethanol has a positive energy output when the fertilizers are produced by modern processing plants, the corn is converted in modern facilities, and farmers achieve normal corn yields. The study estimated that 67,768 BTU of energy is required to produce one gallon of ethanol. The study concluded that corn ethanol is energy efficient because the data showed a positive energy ratio of 1.24. Or, for every BTU dissipated to producing ethanol there was a net 24% energy gain. This is based on assumption that the energy for ethanol is 83,961 BTU 1 [25].

Other more recent studies consider other factors. For example, D. Pimentel in 2003 includes all 50 states in his study instead of just the nine top corn-producing states in the Midwest. Pimentel also includes the environmental impacts of insecticides and fertilizers and takes into consideration the strain on the human food supply created by the demand for ethanol. He further explains that the energy balance of ethanol production is negative (that it takes 29% more energy to produce ethanol than it yields) with the additional costs factored into the energy balance formula. The article also states that profitable utilization of the by-products of ethanol production can help moderate the negative energy balance ratio [26], which was not included in his energy balance equation which partially accounts for the negative energy balance. It is also important to note that his model assumed a higher than normal usage of fertilizer.

1.7 Ethanol production

The production of ethanol or ethyl alcohol from starches and sugar-based feedstocks is a technology that dates back more than 1000 years. While the basic steps remain the same as original technique, the process has been refined over the years. Although this refinement has lead to a relatively efficient process, the industry continues to search for improvements for the overall efficiency and profitability of the plants. For example, some facilities are now utilizing biomass gasification and methane gas digesters to help cut the costs of the natural gas used during production [23].

As indicated in the previous section, there are two different processes for ethanol production: dry milling and wet milling. The biggest difference between the two processes is in the initial treatment of the grain. These two processes are detailed in the following sections.

1.7.1 Dry milling

In dry milling the entire corn kernel is first ground into meal, and processed without separating the component of the grain. The meal is mixed with hot water (+120°C) and a small portion of enzymes in a jet cooker (hydro-cooker) to form mash. This process softens and sterilizes the corn. Additional enzymes are then added to the mash to convert the starch to glucose, a simple fermentable sugar. Ammonia is normally added for pH control and as a nutrient for the yeast. The mash is cooled and then transferred to the fermentation tanks, where yeast is added, and the conversion of starches to sugars is completed, as well as the fermentation of the sugars to ethanol and carbon dioxide. Dry milling process is depicted in Figure 1.8 [62].

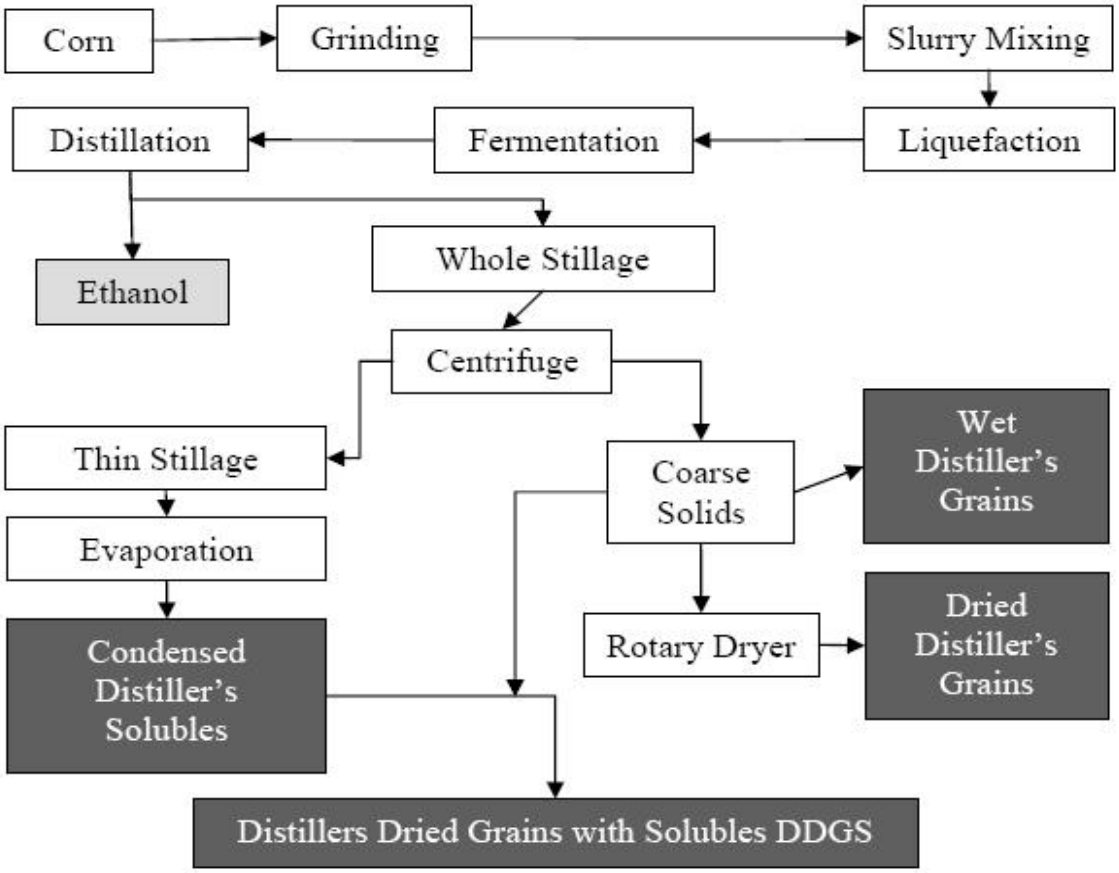

Figure 1.8 Dry milling processes [62]

The fermentation process can take up to 50 hours. During this phase of the process, the mash is continuously agitated and kept at the correct temperature range below 35°C to assist the activity of the yeast. It has been reported that the optimum temperature range is between 32-35°C [60] and at temperatures higher than 35°C the fermentation efficiency significantly decreases [61]. After fermentation the resultant product is transferred to distillation columns, where the ethanol is separated from the remaining stillage. The ethanol is then concentrated to 190 proof (80% wt) by distillation, and dehydrated to approximately 200 proof (100% wt) in a molecular sieve column. The resulting anhydrous ethanol is then

mixed with approximately 5% denaturant, such as gasoline, to make it inconsumable by humans, so it is not subject to alcohol beverage taxes. It is delivered to gas stations or other retailers [23].

The remaining stillage is passed through a centrifuge that separates the coarse grain from the solubles. The solubles are then concentrated to approximately 30 to 50 % solids by evaporation, resulting in condensed distillers solubles (CDS) or syrup. The coarse grain and the syrup are then dried together to produce dried distillers grains (DDG). Usually a portion of the CDS is added to the DDG to improve the nutritional value and the final product is dried distillers grains with soluble (DDGS), and sold as livestock feed. The carbon dioxide that is released during fermentation is typically captured and sold for other uses, such as carbonating soft drinks and beverages, and the production of dry ice [23].

1.7.2 Wet milling

In the wet milling process, the grain is initially soaked in water and diluted sulfurous acid for 24 to 48 hours. This steeping process facilitates the separation of the grain into its components. After steeping, the corn slurry is sent through a sequence of grinders to separate the corn germ. The corn oil from the germ is either extracted during this step, or the germ is sold off to other facilities that extract the corn oil. The remaining fiber, gluten, and starch are further segregated using centrifugal, screen, and hydrochloric separators [23].

The steeping liquor is concentrated in an evaporator. This concentrated product, commonly called heavy steep water, is dried with the fiber component and is then sold as corn gluten feed for livestock. Heavy steep water can also be sold by itself as a feed ingredient. The gluten component, high in protein, is filtered and dried to produce the corn gluten meal coproduct. The starch and any remaining water from the mash can then be processed in three ways. It can be fermented into ethanol, dried and sold as dried or modified cornstarch, or processed into corn syrup. The fermentation process for ethanol is very similar to that used in dry milling, as shown in Figure 1.9 [62].

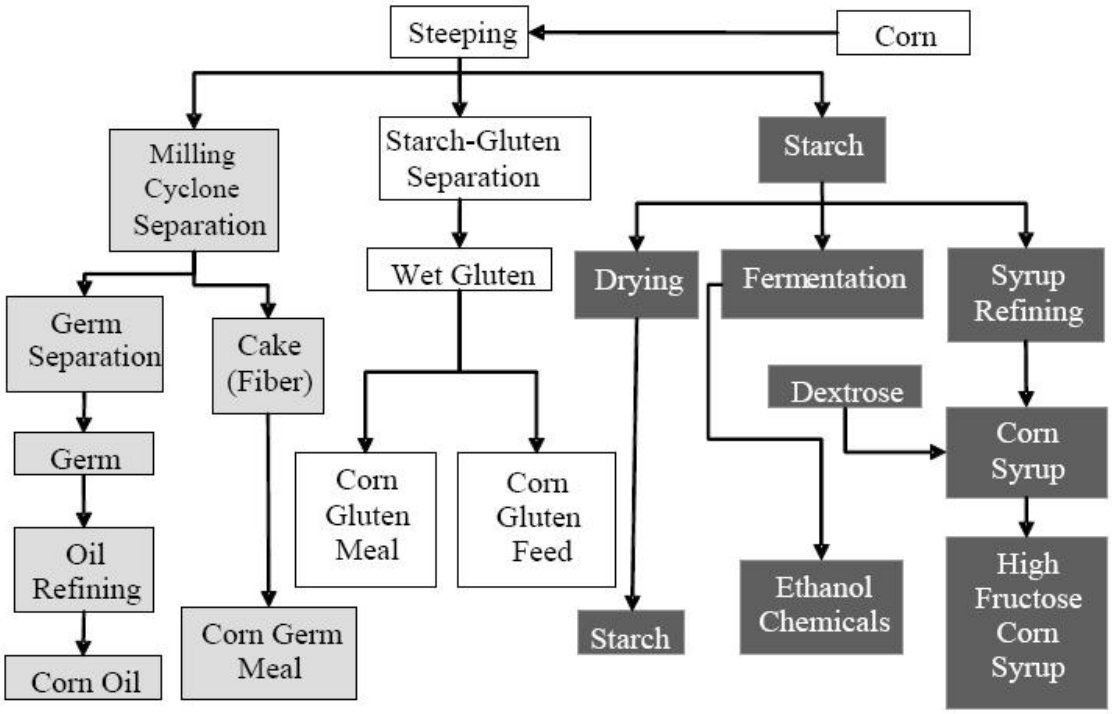

Figure 1.9 Wet milling process [62]

1.8 Anaerobic digestion

Anaerobic digestion is a process that uses microorganisms to break down biodegradable substances in the absence of oxygen. It is commonly used to treat wastewater and break down sewage wastes. The anaerobic digestion process has four essential steps: hydrolysis, acidogenesis, acetogenesis, and methanogenesis. Each of the steps has its own unique type of bacteria. One of the biggest drawbacks to anaerobic digestion is the technical expertise required to properly use and process the bacteria and feedstocks. This, along with high capital costs and lower process efficiencies, are a few reasons why this process has not been widely developed on an industrial scale [27].

During hydrolysis, complex organic polymer chains such as carbohydrates, fats, and proteins are broken down into simple sugars, fatty acids, and amino acids. The second step in this process is acidogenesis. The acidogens convert the resulting sugars, fatty acids, and amino acids into carbonic acids, alcohols, hydrogen, carbon dioxide, and ammonia gas. The third stage of the anaerobic digestion process is acetogenesis. Throughout the acetogenesis process, acetogens further digest the remnants of the previous process into hydrogen, acetic acid, and carbon dioxide. The final stage of anaerobic digestion is methanogenesis. The methanogens finish digesting the hydrogen, acetic acid, and carbon dioxide into methane and carbon dioxide gases. The chemical reaction for the entire anaerobic digestion, which converts complex sugars and carbohydrates into carbon dioxide and methane gas, is $C_6H_{12}O_6 \rightarrow 3CO_2 + 3CH_4$ [27].

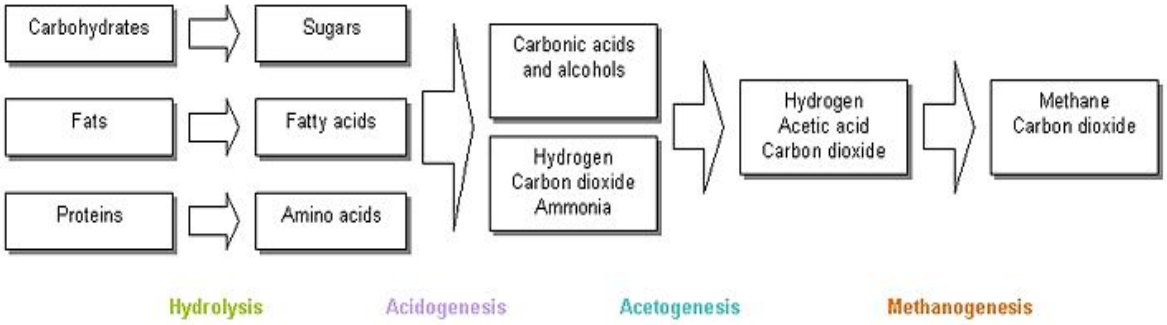

Figure 1.10 Anaerobic digestion stages [27]

1.9 Ultrasonics

Ultrasound is defined as sound waves that are above the audible hearing range of humans, typically greater than 18 kHz, with most of the practical higher power applications falling in the 20-60 kHz range. [28] Low power ultrasound is commonly used in electronic, navigational, industrial, security applications, and in medicinal applications [29].

Low power ultrasound can also be used for imaging because the high frequency acoustic waves reflect off objects. The distance to an object can be determined by measuring the time between the transmission of an ultrasound pulse and the return of the echo. Bats use this ultrasound technique to find their way during the night and hunt for food. Marine animals such as dolphins and whales are also believed to use this technology. Ultrasound also can be used in maritime sonar systems to determine the depth of the water in a specific location, to find groups of fish, to locate submarines, or to detect scuba divers [29].

Figure 1.11 Ultrasound [30]

Another good example of the use of ultrasonic frequencies is an ultrasonic detection system. Its constant high frequency acoustic signals are transmitted by a group of transducers. The ultrasonic waves inundate the area that is being monitored by the system. The receiving transducers check the ultrasound reflected by objects in the field. If movements or changes in the area produce a variation in the phase of some of the reflected waves that go back to the receivers, this phase change is detected and then sends signals to sound the alarm system. Such ultrasonic security systems are popular among car owners. Other applications of ultrasound are in medical imaging (shown in Figure 1.11), where the high frequency acoustic energy is transmitted into the human body by transducers that are placed on the skin. The ultrasound waves reflect off organs and surrounding fluids in the body and between areas of differing tissue density. This is mostly used to monitor the condition and behavior of fetuses preceding birth. It can also be used to locate tumors or cancerous legions and to examine the condition of muscles and bones in the body. Ultrasound can be used in industry to evaluate the consistency and purity of liquids and solids. It can also be used for ultrasonic cleansing purposes. [29]

1.9.1 Background

The conversion of electrical energy into mechanical vibrations is critical for efficient ultrasonic production. This is typically achieved in a transducer. The transducer converts the electrical energy to mechanical energy. A common design of a transducer is a piece of polarized material that has electrodes attached to its positive and negative faces. When an electric field is applied across the material, the polarized molecules align themselves with the electric field, causing the material to change dimensions. This phenomenon is known as electrostriction. A permanently polarized material such as quartz (SiO_2) or barium titanate ($BaTiO_3$) will produce an electric field when the material changes dimensions as a result of an imposed mechanical force. This is known as the piezoelectric effect [31].

The active element of most acoustic transducers used today is a piezoelectric ceramic. Prior to the development of piezoelectric ceramics in the early 1950s, ceramic nonferrous piezoelectric crystals made from quartz and magnetostrictive ferrous materials were primarily used, and the active element is still often referred to as the crystal. [31].

Magnetostrictive ferrous materials change shape in the presence of a magnetic field, converting the energy in a magnetic field into mechanical energy, while piezoelectric materials change shape (show in Figure 1.12) by converting the electrical energy into mechanical energy when an electric voltage is applied through it. The inverse is also true in piezoelectric materials; when a mechanical force is applied, it will produce an electric voltage. Piezoelectric systems also transfer energy more efficiently compared to

magnetostrictive systems due to the direct transfer of energy. In more detail, a magnetostrictive system must transfer energy from electrical to magnetic, and then into mechanical energy. [59]

After piezoelectric ceramics were introduced, they became the major material for transducers due to their high efficiency and their ease of manufacture into a variety of shapes and sizes. The first piezoceramic in common use was barium titanate, and that was followed during the 1960s by the lead zirconate titanate compositions that are now the most commonly employed ceramic for making transducers. New materials such as piezopolymers and composites are also being used today [31].

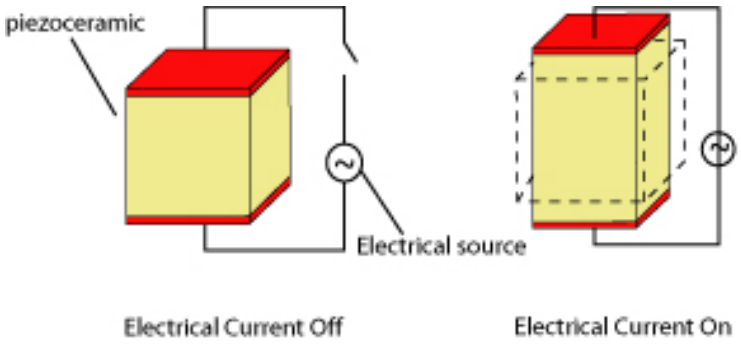

Figure 1.12 Piezoceramics [31]

The thickness of the active element is determined by the desired frequency of the transducer, as well as selected voltage available from the power supply. There are limitations though, as the higher the frequency of the transducer, the thinner the active element. [31]

1.9.2 High power ultrasonics

In contrast to low power applications, high power ultrasonic applications use lower frequencies typically in the range of 20 to 100 kHz [32] because the power is constrained by the heat limitation on an ultrasonic system when using higher power. The maximum available power of a system is limited by the capacity of the ultrasonic transducer .In more detail, in order to maintain resonance, maximum available power is inversely proportional to frequency as detailed Figure 1.13. [58]

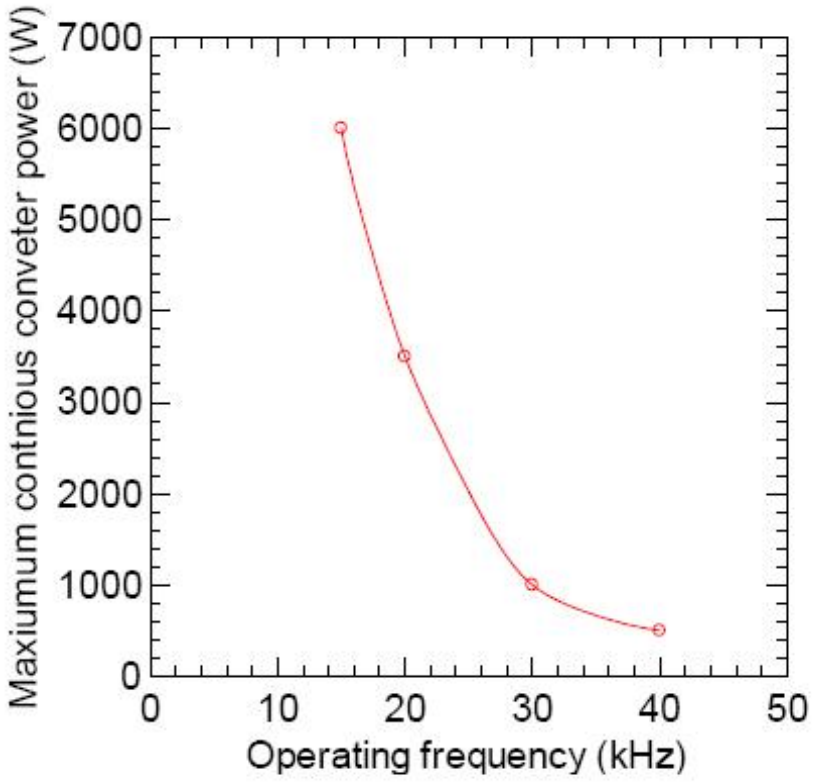

Figure 1.13 Maximum available power as a function of frequency [58]

Typical operating frequencies for high power applications are 10, 15, 20, 25, 30, 35, and 40 kHz. Systems with a frequency between 20-30 kHz are a good compromise, maintaining a relatively high power without sacrificing frequency significantly. [58]

1.9.3 Cavitation

When high power ultrasonics is applied through a medium such as water, cavitation due to ultrasonic rarefaction occurs. These low-pressure cavities implode violently, causing the surrounding particles in the solution to break apart due to the intense hydromechanical shear forces in the solution [33]. In more detail, the magnitude of the negative pressure in the areas of rarefaction eventually becomes sufficient to cause the liquid to fracture producing bubbles [34].

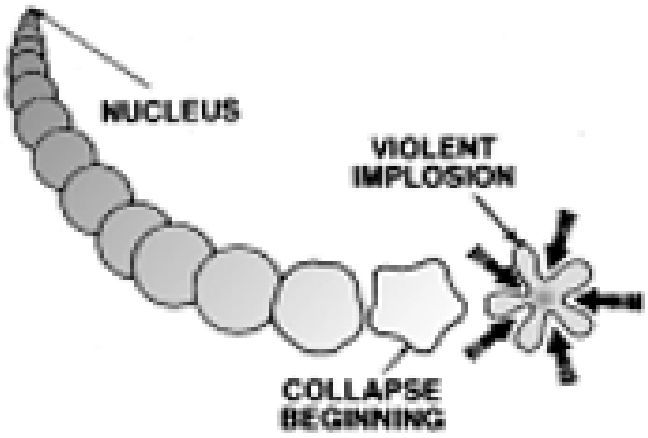

Figure 1.14 Cavitation bubble collapse [35]

Cavitation "bubbles" are typically created at nucleation sites such as impurities or interfaces. As the liquid fractures or tears because of the negative pressure of the sound wave in the liquid, the liquid is vaporized. As the wave fronts propagate, the cavitation bubbles oscillate under the influence of positive and negative pressure and eventually grow to an unstable size. The violent collapse of the cavitation bubbles results in implosions, which cause shock waves and jets radiated from the sites of collapse [34].

1.9.4 Acoustic streaming

Another phenomenon that occurs in a nonelastic medium such as water, when exposed to ultrasonic energy is acoustic streaming [34]. Acoustic streaming is the phenomenon caused by high frequency sound waves when present in a fluid [36]. This is also called acoustic flow [37]. When ultrasonic waves are applied through water, the temperature of the liquid and any solid object in it increases. The origin of this increase in heat transfer is due to the agitation effect from the microjets of cavitation shearing and from acoustic streaming [38]. It has been found in recent studies that the acoustic streaming velocity is proportional to the square of the vibration amplitude [39].

In a similar study, it was determined that acoustic streaming velocity is determined by the properties of the fluid such as acoustic attenuation (loss of intensity), viscosity, sound velocity, time of exposure, frequency, aperture size, and pressure amplitude. It has been theorized that acoustic streaming velocity increases when amplitude, attenuation, and

frequency increases, and when aperture (opening) size decreases. It was further found that acoustic streaming velocity decreases when the fluid viscosity increases [40].

1.9.5 Resonance

In mechanical terms, resonance is the tendency of a system to oscillate at maximum amplitude with least amount of driving force and occurs at certain frequencies. Because the system stores energy at these frequencies, smaller forces can produce large amplitude of vibrations. Resonance can occur with a wide range of energy including mechanical, and electromagnetic waves [41].

Many objects usually have more than one resonance frequency, as well as associated harmonics for each mode of resonance. A system will vibrate at those fundamental resonance frequencies, and vibrate less at the harmonic frequency. Acoustic resonance is also a common consideration in many designs but most evident in the design of acoustical instruments. These resonators are for example, the strings and body of a violin, the length of a flute, or the shape of a drum [42]. In contrast, a classic example of an undesired resonance was the destruction of the Tacoma Narrows Bridge in Tacoma, Washington on November 7, 1940 [43].

1.9.6 Equipment

1.9.6.1 System and components

There are four main components to an ultrasonic system: the power supply, the converter, booster, and the horn. The power supply converts the input electrical power to the current, voltage, and frequency that the system requires. The converter, or transducer, converts the electrical power into mechanical vibrations at the resonant frequency. The motion/strain within the transducer is produced by piezoelectric disks, which are held together by high tensile strength bolts. The booster, a mechanical amplifier, which is optional, is commonly used to increase the vibration amplitude of the system. The last component of the system, the horn, which comes in a variety of shapes and sizes, is dependant on the application [44].

The peak to peak amplitude can be estimated by multiplying the four factors of the ultrasonic stack, namely the percentage of the controller amplitude and the converter's rated amplitude with the gain of the booster and the horn that are detailed in Figure 1.15.

Example: $(100\%\,Amplitude)\times(0-20\mu\mathrm{m}\,Converter)\times(1:1 Booster)\times(1:8 Horn)=$

$(1)\times(20)\times(1)\times(8)\ = 160\ \mu\mathrm{m}_{pp}$

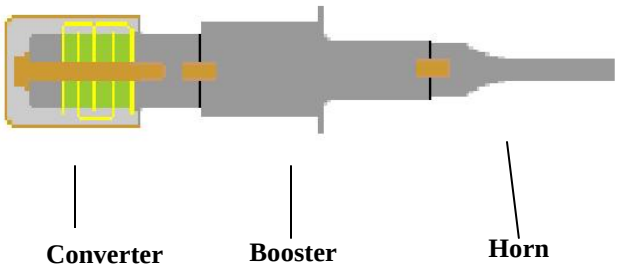

Figure 1.15 Ultrasonic unit assembly [44]

1.9.6.2 Tooling

Industrial ultrasonic tooling manufacturers will typically design and build both custom and standard ultrasonic horns (examples shown in Figure 1.16) for use on all brands of ultrasonic systems [45]. These horns are often called the tooling.

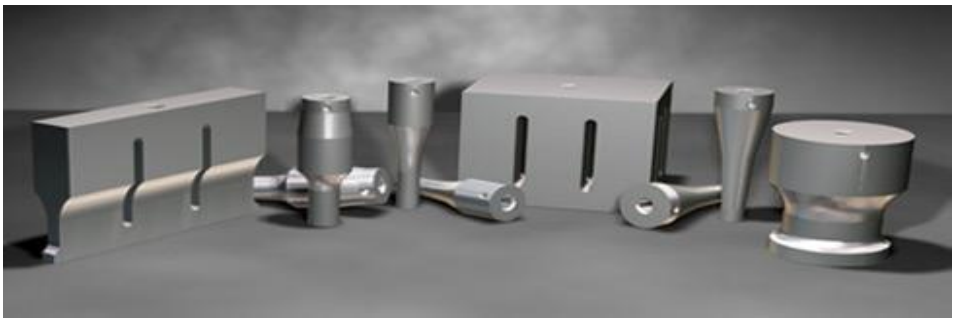

Figure 1.16 Ultrasonic horn varieties [45]

There are many typical applications for ultrasonic tooling, including but not limited to welding, inserting, spot welding, de-gating, staking, liquid treatment, cleaning, cutting, machining, scientific experimentation, and textile cut, and sealing. Ultrasonic tooling can

also be made for specific frequencies ranging anywhere between 1 and 100 kHz, but preferably for 20 kHz, 30 kHz, or 40 kHz. The ultrasonic horns are also made in a wide range of shapes, including rectangular, rectangular slotted, circular, circular slotted, circular hollow, catenoidal, and exponential. Ultrasonic horns are typically made from aluminum, titanium, hardened powdered steel, or hardened tool steels. Horns can also be anodized or coated in chrome plating, titanium nitride, or other materials to increase the wear resistance, preventing oxidation on aluminum horns or rust on steel horns. Tooling is generally customized to the application of the ultrasonic device itself [45].

1.10 Optical microscopy

Optical or light microscope is a type of microscope that uses a series of lenses and visible light to magnify small objects (see Figure 1.17.) They are the oldest and the simplest types of microscopes. Early versions of simple optical microscopes consisted of a single lens such as the versions made by famed scientist Antonie van Leeuwenhoek. While the single convex lens types are now considered obsolete, they are still used for other magnification devices such as magnifying glasses and loupes. The compound microscope, a light microscope that utilizes more than one lens, was developed in the late 1500s to the mid-1600s. While van Leeuwenhoek is often credited with the development of the first compound microscope, other scientists such as Dutch spectacle makers Hans and Zacharias Janssen and astrologer Galileo Galilei also experimented with the use of multiple convex and concave lenses in series [46].

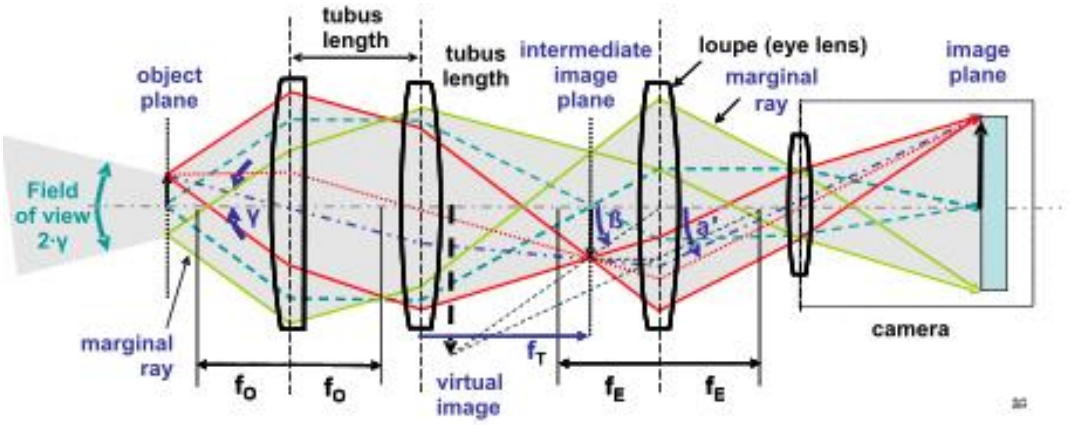

Figure 1.17 Optical microscope conceptual components [46]

Modern optical microscopes have sets of objective lenses (typically 4x, 5x, 10x, 20x, 40x, 80x, and 100x magnification) and a set of eyepiece lenses (typically 2x, 5x, and 10x magnification). The final magnification of the object is obtained by simply multiplying the objective lens magnification to the eyepiece magnification. The image of the object being observed is viewed though the series of the selected lenses with the illumination of the object provided, either by a natural light source and a reflective mirror, or by an artificial source from a bulb [46].

1.11 Scanning electron microscopy

The scanning electron microscope (SEM) is an electron microscope that images a sample's surface by scanning it with a beam of electron particles in a raster scanning pattern in a vacuum chamber rather than using light to create the image (see Figure 1.18.) Modern SEMs typically have a magnification from approximately 25 times to 250,000 times the original sample's size. The first SEM image was obtained in 1935 by scientist Max Knoll, and this concept was further developed and patented by British scientist Manfred von Ardenne in 1937 and later by Professor Sir Charles Oatley in 1965 [47]. In a standard SEM, the electrons are emitted by a tungsten filament cathode and accelerated towards the anode through the magnetic lens to the sample. The electron beam hits the sample and it emits primary electrons, secondary electrons, and x-rays, which are collected and converted into a signal that produces the image [48].

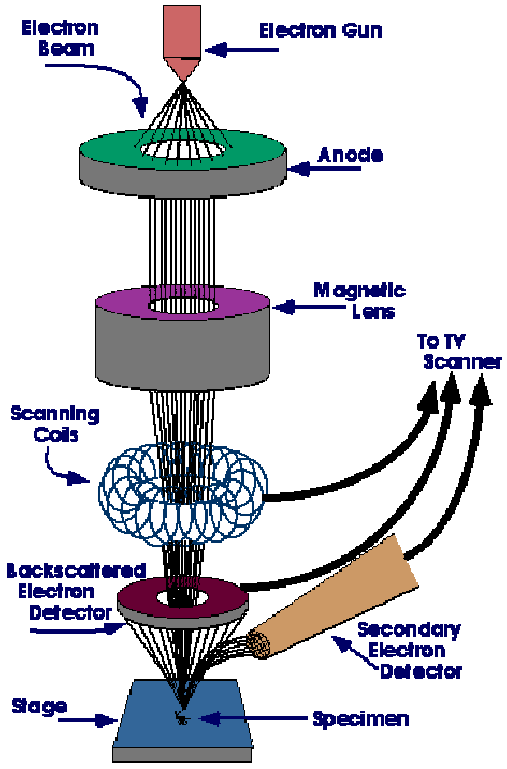

Figure 1.18 SEM conceptual components [48]

Non-electrically conductive samples (such as biological sample) must be coated with an electrically conductive material before they can be imaged with a standard SEM system. This coating will ensure that the electrons have a path to be grounded. A coating such as gold, gold/palladium alloy, platinum, tungsten, or graphite is deposited on the sample either by low vacuum sputter coating or by high vacuum evaporation. In the 1980s environmental scanning electron microscopes (ESEMs) were developed that allowed samples that were not electrically conductive to be observed without coatings. This is due to the sample chamber being at a higher pressure than the vacuum in the electron optical column. The pressure and the type of gas in the chamber can be controlled as needed [47].

1.12 Particle distribution analysis

Particle distribution analysis is the measuring and quantifying of a granular/powdered sample or dispersed particles, and is often completed in a fluid. It is also known as particle size distribution (PSD) analysis. There are many types of PSD analysis, the simplest being sieve analysis. Sieve analysis uses a series of sieves to examine the percentage of particles that fall through consecutive smaller sieve range. There are disadvantages to this technique: not all particles are a perfect spherical shape, and the smallest practical sieve size ranges from 20 to 40µm. Other types of PSD analysis include automated optical counting using electron micrographs, as well as the coulter counter, sedimentation, and laser diffraction. The coulter counter determines the number of particles by measuring the changes that occur in the conductivity of a liquid passing though an orifice and tabulating the pulses of back pressure that occur when particles in the liquid pass through the orifice. In the sedimentation technique, the particles are suspended in a liquid, and the optical density of each layer of particles is measured. In laser diffraction, the diffracted light pattern is produced when the laser beam passes through a dispersion of particles in air or in a liquid. As the particle sizes increase, the angle of diffraction decreases. Modern electronic equipment measures the angle of diffraction, and can calculate a continuous measurement of the particles. Laser diffraction PSD is highly accurate and can measure particles smaller than 1 µm. Laser diffraction has now become the dominant procedure for measuring PSD [49].

1.13 Research questions

The research questions that will be answered in this thesis are:

1) What are the effects of ultrasonic treatment on selected dry mill ethanol co-products?

2) How much of a reduction in particle size is realized in ultrasonic treatment of these co-products?

3) Is there a difference in particle size reduction of the various co-product types?

4) What are the changes in morphology of the various coproducts after ultrasonic treatment?

1.14 Objective

The objective of this research was to determine the effects of the various ultrasonic treatment exposures on the selected dry mill ethanol production coproducts by analyzing and observing the treatments with optical imaging microscopy, scanning electron microscopy, and particle size analysis. The vision of this research is to improve biogas production by various ultrasonic treatments (amplitude and time) of selected dry mill ethanol production coproducts and promoting anaerobic digestion for enhanced biochemical methane production (BMP).

CHAPTER 2: METHODS

2.1 Sample extraction

The coproducts analyzed in this study were collected from the Lincoln Way Energy ethanol production facility located in Nevada, Iowa [22]. The coproducts studied were (1) DDGs, (2) solids, (3) syrup, and (4) thin stillage, and the collection locations are detailed in Figure 2.1.

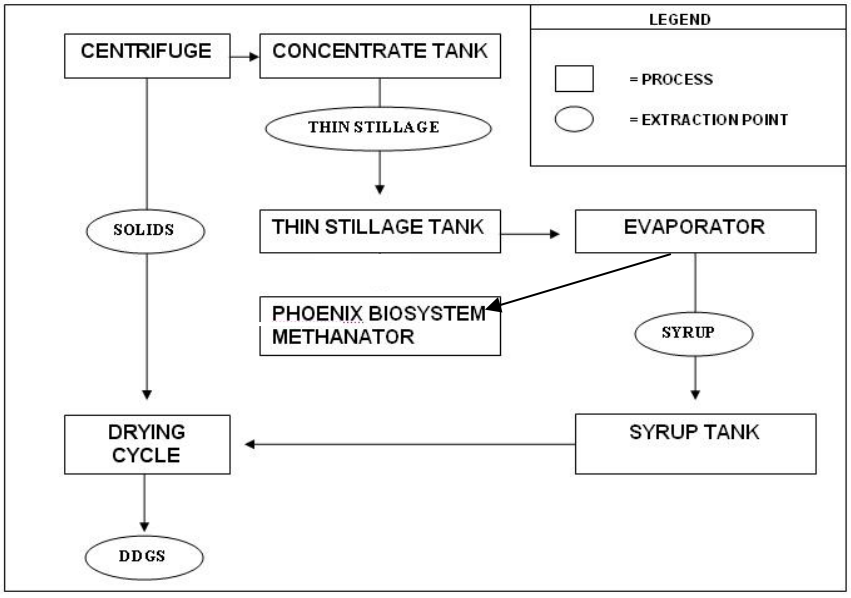

Figure 2.1 Extraction points [22]

2.2 Sample preparation

The four samples were treated using a 2.2 kW, 20 kHz Branson 2000 series ultrasonic unit [50] with a 1:1 gain booster and a 1:8 gain titanium catenoidal horn with a 10 mm diameter face. Figure 2.2 shows the ultrasonic treatment setup used for experimentation.

Figure 2.2 Experimental setup

Screening experimentation indicated that a maximum of 3 g of DDGs, solids, and syrup was allowable in a 35 ml volume of water in a plastic 50 ml tube to achieve uniform ultrasonic treatment as shown in Figure 2.3. Higher solid levels resulted in poor mixing during treatment. The catenoidal horn was lowered into the vial to the 15ml line. After the samples were treated, the horn was cleaned and submersed into cool water before running other sample types. The treatments were completed at three different amplitudes, 33% (52.8 μm_{pp}), 66% (105.6 μm_{pp}), and 100% (160 μm_{pp}), and five treatment times, 10, 20, 30, 40, and 50 s.

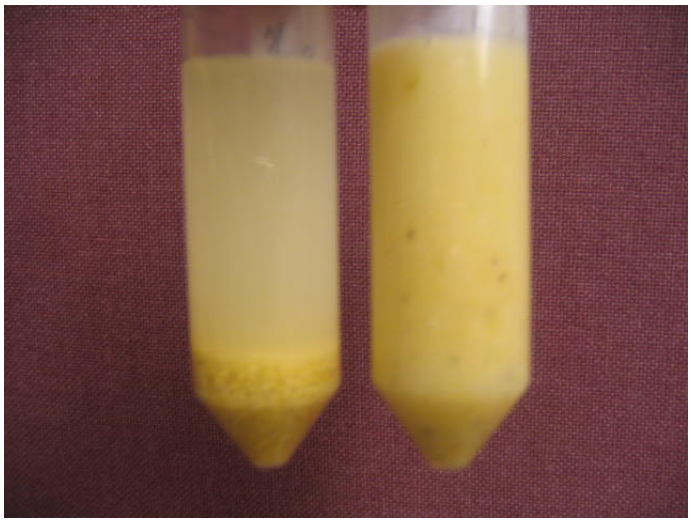

Figure 2.3 Untreated and treated sample in 50 ml tube

A subset of the experimental design, detailed in Figure 2.4, was chosen for the optical microscopy imaging (OM), scanning electron microscopy imaging (SEM), and particle distribution analysis (PDA). Treatments of 10 s at amplitude of 52.8 μm_{pp}, 50 s at amplitude of 52.8 μm_{pp}, 10 s at amplitude of 160 μm_{pp}, and 50 s at amplitude of 160 μm_{pp} were performed for the characterization study. The BMP tests conducted to determine the biogas yield from the control and ultrasonically pretreated coproducts are reported in a related paper [51].

Amplitude (μm_{pp})	Time (s)
160	10, 50
52.8	10, 50

Figure 2.4 Treatment matrix for OM, SEM, and PDA

To observe the effects of the sonication, OM images at three magnifications (10x, 20x, and 40x) were captured using the Aixo Imager 2 imaging system attached to the Zeiss Compound Microscope for the DDGs and solids sample types [52]. For the thin stillage and syrup sample a Nova Vision Series microscope was used at three magnifications (10x, 40x, and 100x), and images were captured with a Cannon SD110 Powershot digital camera attached to the optical lens.

Figure 2.5 Optical microscope

A Hitachi S-2460N variable pressure scanning electron microscope was used for SEM imaging [53]. Images were captured at 7x, 20x, 100x, 300x, and 1000x magnification with the Oxford Instruments "Isis" energy-dispersive x-ray system [54], which was attached to the SEM. Because this is variable pressure system, precoating of the samples was not required and direct imaging of the substrates was possible.

Figure 2.6 Hitachi S-2460N SEM

Particle distribution analysis (PDA) was completed using dry samples (DDGs and solids) that were screened through a sieve to remove particles larger than 1000 µm because of the limitations of the Malvern Mastersizer 2000 PDA system [55]. The DDGs samples were sifted through a 500 µm No. 35 sieve; however, due to the higher moisture content of the solids, a larger No. 20 sieve was used for the solids. Approximately 30-40% of the solid particles fell through the sieve for the solid sample types. The syrup and the thin stillage particle sizes did not require sieving.

Figure 2.7 Sieving solid samples

Figure 2.8 Malvern Mastersizer 2000 PDA

CHAPTER 3: RESULTS AND DISCUSSION

3.1 Optical microscope imaging

After the samples were treated, it was observed that there was a significant difference between the treated and the control samples (no ultrasonic treatment). For example, after treatment gravity settling resulted in three visible layers that appeared to have varying densities, while in contrast, the control group only exhibited a single layer. Microscopic evaluation confirmed that each layer correlated to various particle sizes. Figures 3.1 and 3.2 show optical micrographs images at 40x magnification of untreated and treated samples of the DDGs. Comparing the control to the treated sample, it is seen that the particles were broken apart by the ultrasonic treatment. In more detail, it is seen that cell destruction and remnant debris are scattered (Figure 3.2) when the samples are treated with ultrasonics.

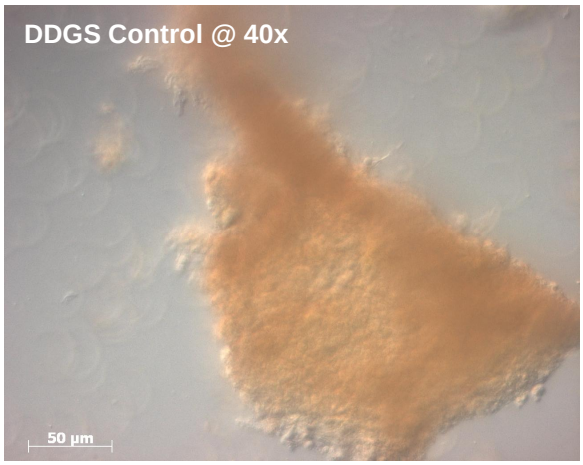

Figure 3.1 DDGs control

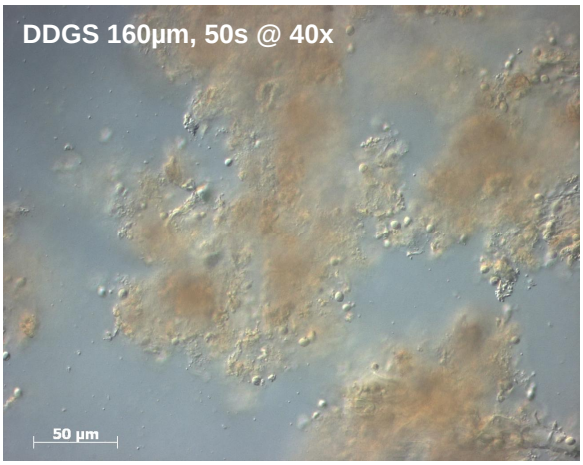

Figure 3.2 DDGs treated

Figures 3.3 and 3.4 shows the images of the solids of the control and the treated sample, respectively, at 40x magnification. While the particle destruction is not as apparent as in the DDGs images above, it is seen that the treated sample exhibited more and smaller lipid droplets. In more detail, in the treated sample the lipids are more abundant and are noticeably smaller in size compared to the control. This observation is most likely related to emulsification often seen with ultrasonic treatment of discontinuous liquid phases.

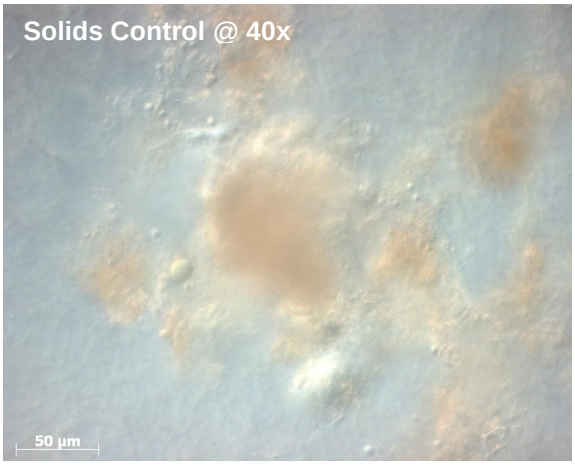

Figure 3.3 Solids control

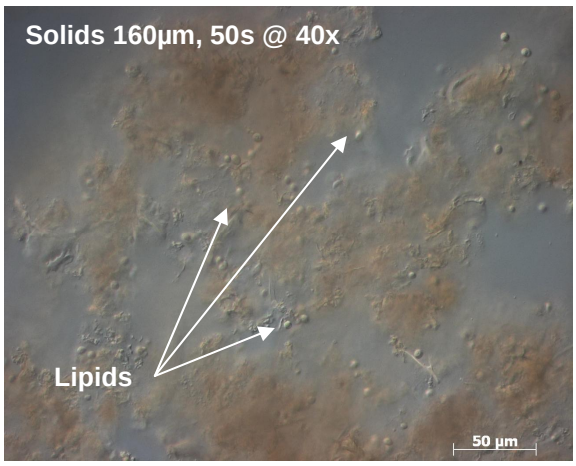

Figure 3.4 Solids treated

Figures 3.5 and 3.6 show the control and the treated samples of the syrup at 40x magnification, and Figures 3.7 and 3.8 show the control and treated samples of the thin stillage at 40x magnification. It should be noted that the particles appear larger in size for the syrup and thin stillage treated samples compared to the control group. While the particles themselves are broken down during ultrasonic treatment, it is speculated that during treatment they bind together or flocculate. This increase in particle size may also be the result of oils being released during sonication and the droplets coalescence after treatment

into larger droplets. These findings, an increase in particle, were not expected and conclusively not fully understood at this time.

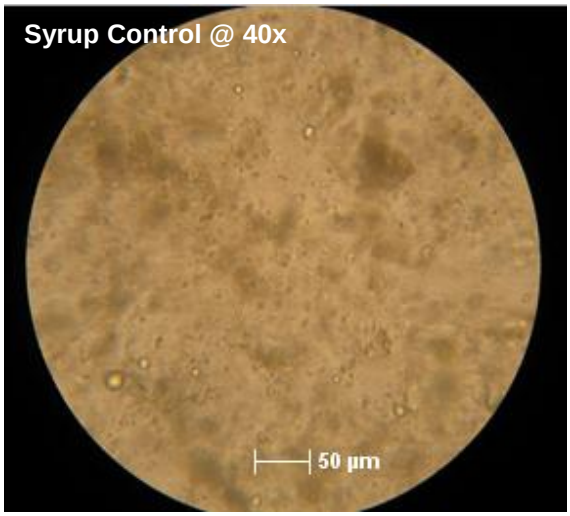

Figure 3.5 Syrup control

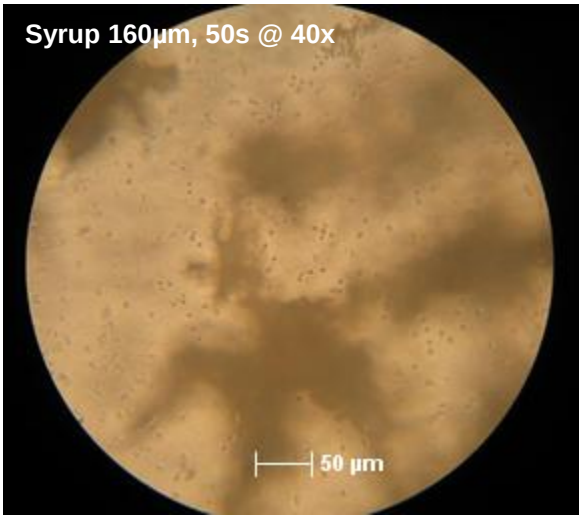

Figure 3.6 Syrup treated

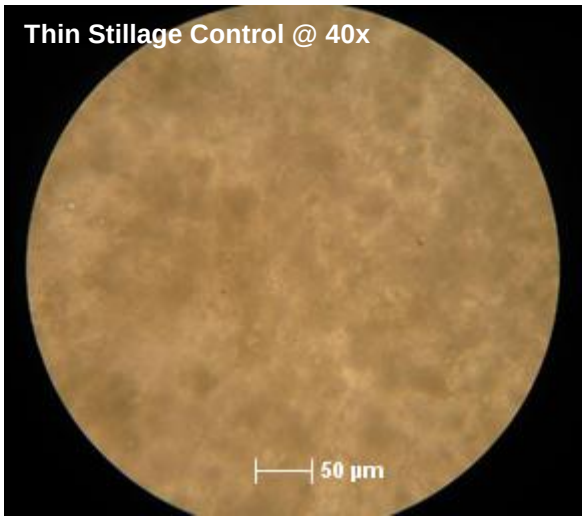

Figure 3.7 Thin stillage control

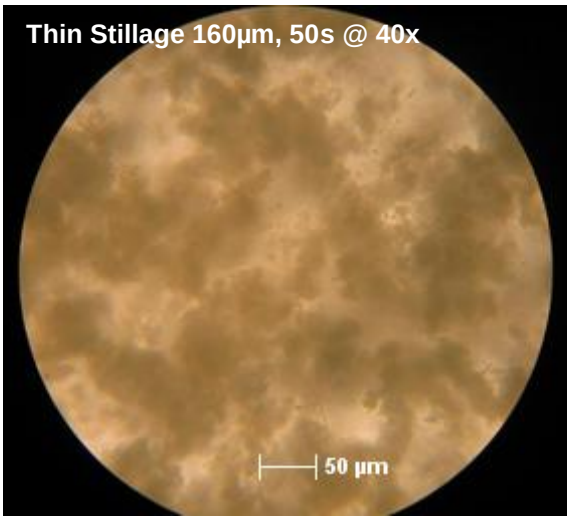

Figure 3.8 Thin stillage treated

3.2 Scanning electron microscope imaging

The SEM images of the DDGs revealed similar results as seen with the optical imaging, as seen in Figure 3.9. In more detail, Figure 3.9 shows the control group, where the DDGs appear to be relatively intact. That is, the cell walls are intact, and the cell cytoplasm and other cell interior morphologies are located inside the cells. In contrast, in the treated sample (160 µm, 50 s) the cell walls are fragmented and contain porous features most likely due to ultrasonic cavitation, as seen in Figure 3.10. Figure 3.11 shows the DDGs control group at 300x magnification, and Figure 3.12 shows the treated sample (160 µm, 50 s). Again, it is seen that cell destruction is prominent in the treated sample as a result of the cavitation produced by ultrasonics, and the results are similar to those reported by others [56]. It should be noted that after sonication, the hull particles of the DDGs were destroyed (compare Figures 3.11 and 3.12), and many of the lipid droplets are scattered and smaller in size.

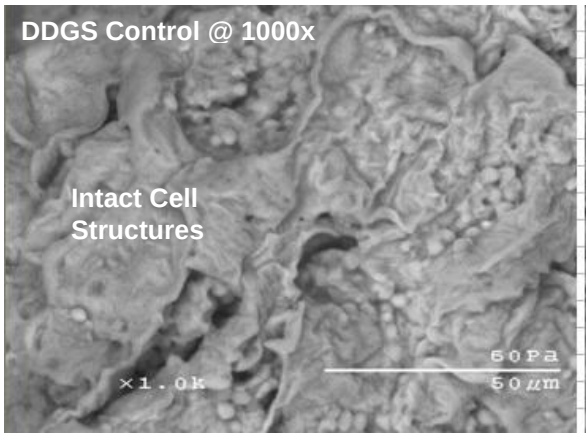

Figure 3.9 SEM of DDGs control

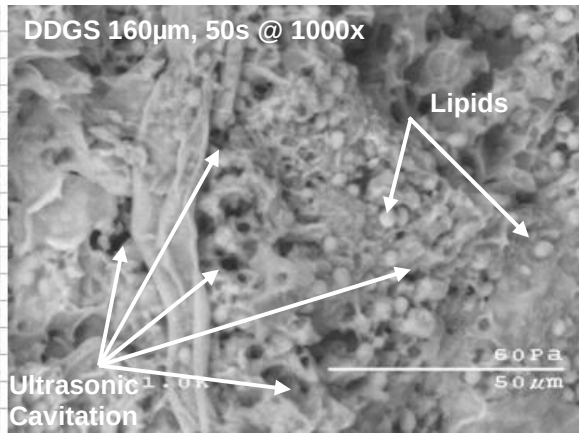

Figure 3.10 SEM of DDGs treated

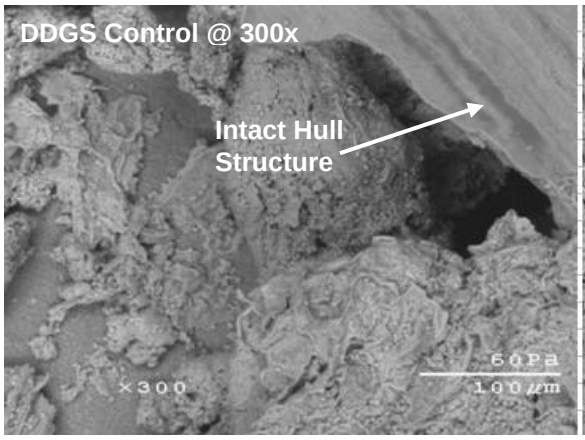

Figure 3.11 SEM of DDGs control

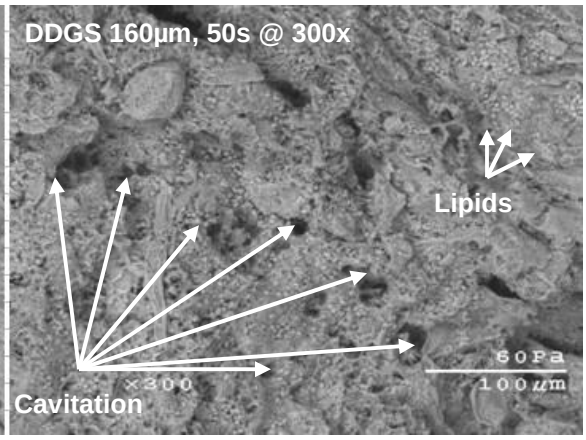

Figure 3.12 SEM of DDGs & Cavitation

Figure 3.13 shows the SEM images for the solids control group at 20x magnification. It is important to note that the particles are relatively intact, in contrast to the ultrasonically treated sample (160 µm, 50 s) shown in Figure 3.14. The particles appear to be noticeably smaller, consisting mostly of powder-like granules with a few of the larger particles remaining. It is believed that the powder-like substance is residual cell fragments. Figure 3.15 shows the solids control group at 1000x magnification. It is important to note the distinct cavities/pores present in the cell walls in Figure 3.15, but not present in Figure 3.16.

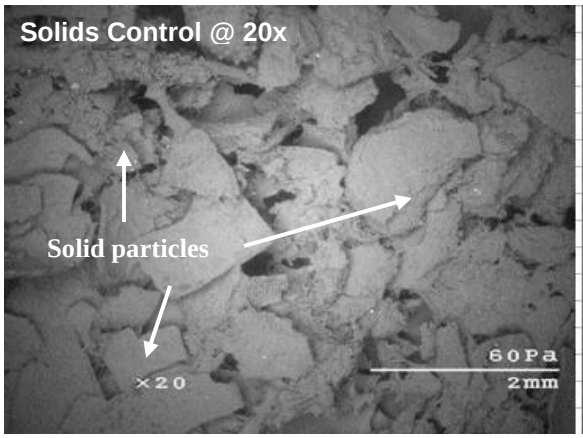

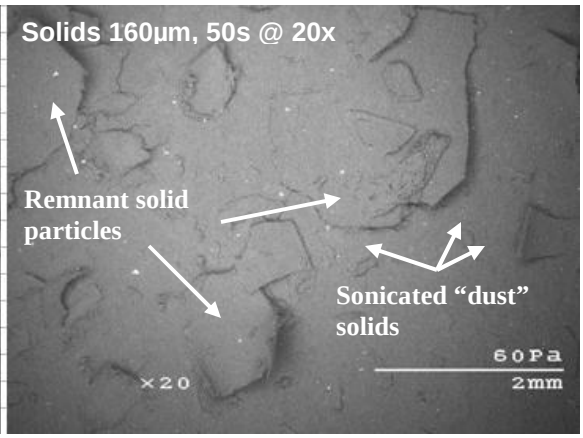

3.13 SEM of solids control

3.14 SEM of solids treated

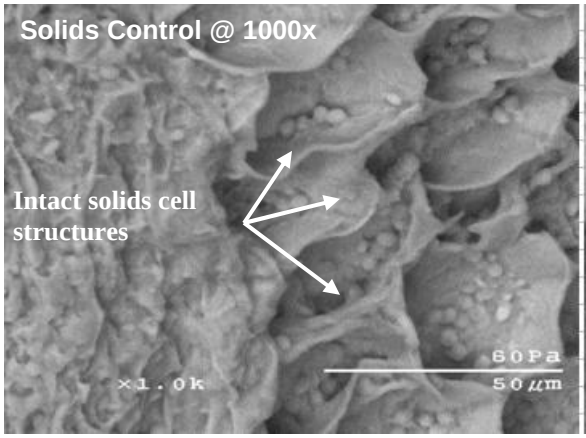

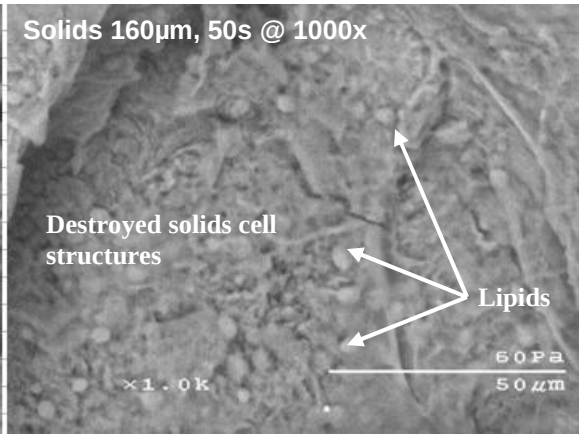

Figure 3.15 SEM of solids control

Figure 3.16 SEM of solids treated

Figure 3.17 shows the SEM image of the syrup control sample at 1000x, and the ultrasonically treated sample (160 µm, 50 s) at 1000x is seen in Figure 3.18. Figure 3.19 shows the thin stillage control sample at 1000x, with the treated sample (160 µm, 50 s) at 1000x magnification shown in Figure 3.20.

These images suggest there is little difference between the control and treated samples. That is to say, there is no visible difference between the treated and control groups

for the thin stillage and syrup samples. While both treated samples appear to have some evidence of pores, that maybe the result of cavitations; however, based on their limited number and size, it is difficult to conclude that they were produced by the treatment.

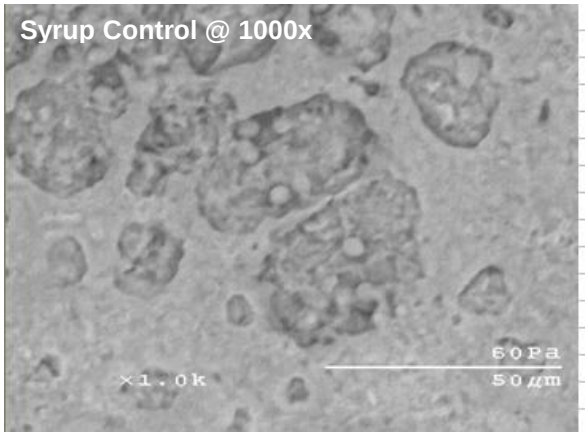

Figure 3.17 SEM of syrup control

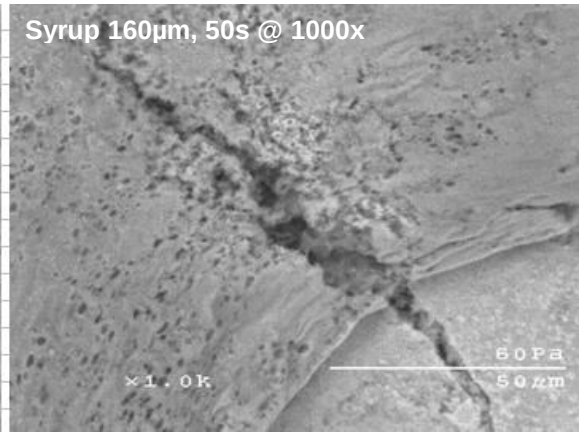

Figure 3.18 SEM of syrup treated

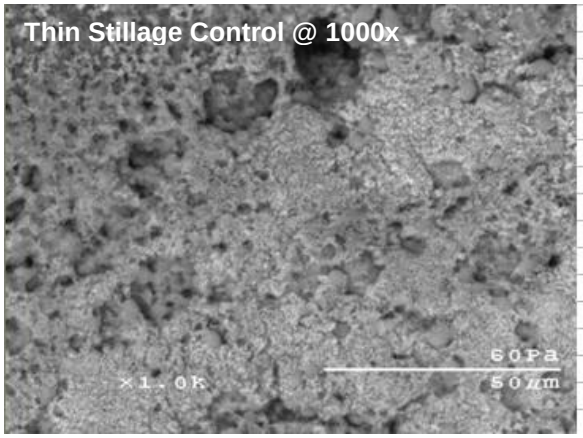

Figure 3.19 SEM of thin stillage control

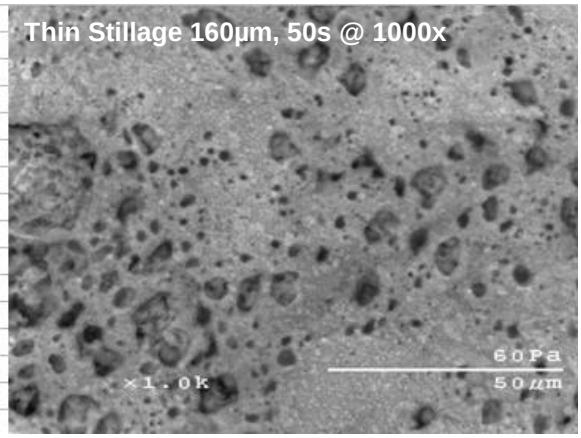

Figure 3.20 SEM of thin stillage treated

3.3 Particle distribution analysis

Statistical data generated by the Malvern Mastersizer software was utilized to create distribution plots for PDA analysis (Figures 3.21-3.24). In most cases, the distribution plots indicate reduction in particle size by ultrasonic treatment compared with the untreated sample (control group). For example, as seen in Figure 3.21, there is a peak population near a particle size of 800 µm for the untreated sample (control). However, with increasing treatment (time and amplitude), the peak population is reduced and shifted to the smaller particles. It is also interesting to note that a tri-nodal distribution of the DDGS is seen. It is believed that this is due to the morphology and fundamental composition of the substrate. For example, the peak at 20-40 µm may correspond to residual starch granules or protein structures.

As seen in Figure 3.22, similar results are obtained with the solids. However, for the syrup and thin stillage samples, as seen in Figures 3.23 and 3.24, the PDA data converged to a more uniformly distribution with increasing treatment (time and amplitude). It is also interesting to note that there is a slight increase in peak particle size, shown by the shift of the curve's peak to the right (larger size). While there is no evidence, it is theorized that the smaller particles are agglomerated by the ultrasonic treatment through high-speed impacts, similar to the behavior observed with metal spheres [57]. As previously noted, this may also be the result of oil droplets coalescencing to form larger droplets, and this oil is released by the ultrasonic treatment.

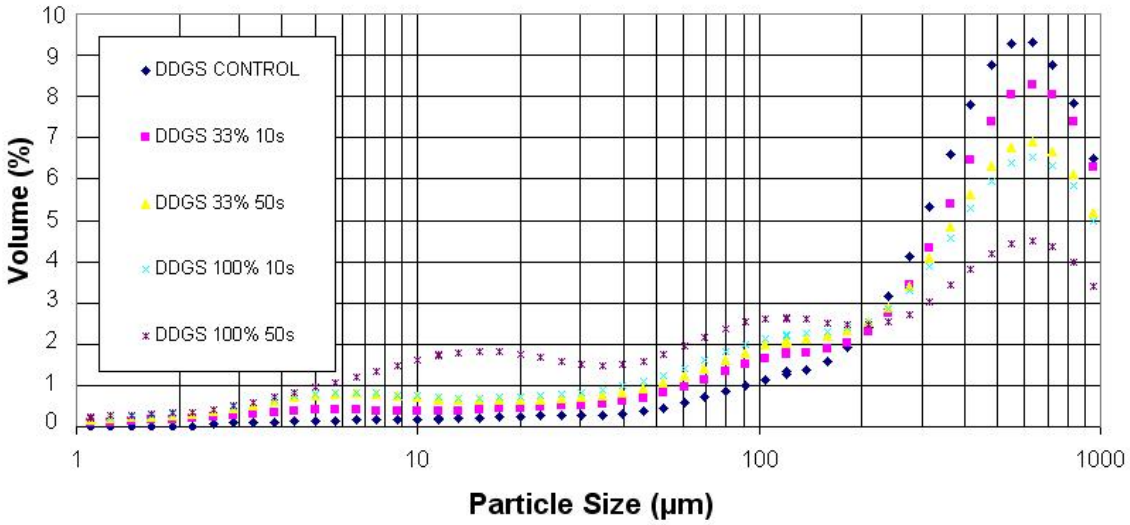

Figure 3.21 DDGs PDA graph

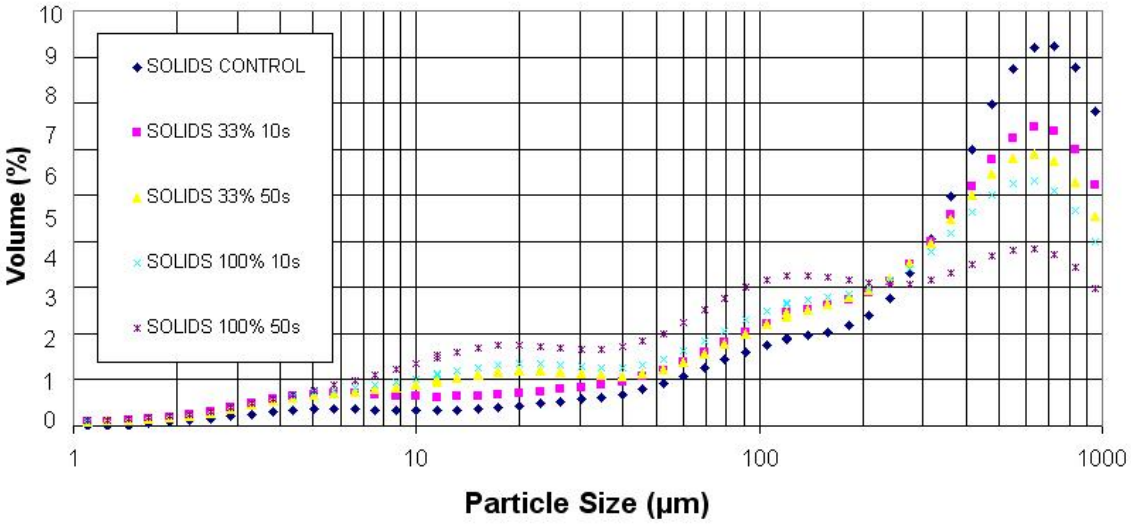

Figure 3.22 Solids PDA graph

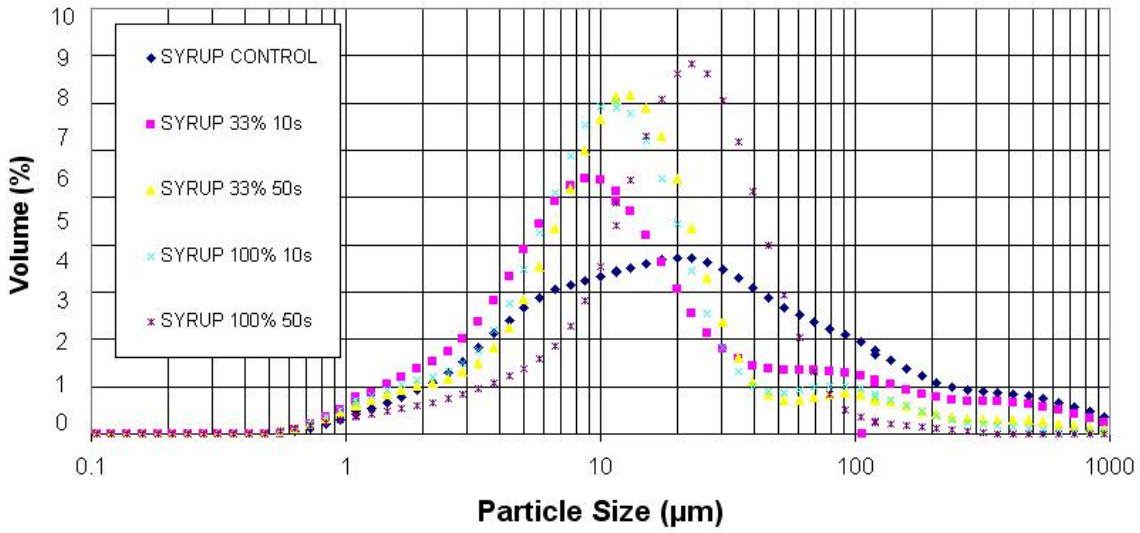

Figure 3.23 Syrup PDA graph

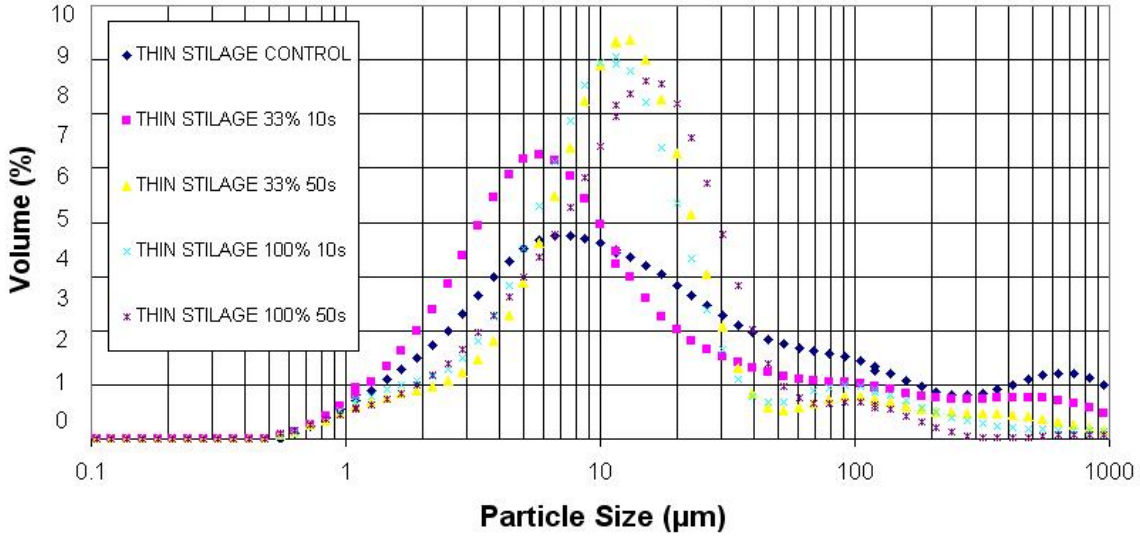

Figure 3.24 Thin stillage PDA graph

After the data was collected, the Malvern software calculated the mean particle size of each treatment. These 3 means were averaged and compared to each other, using a t-test to verify their significance. The p-value chart, null and alternative hypothesis are detailed in Figure 3.25. In each comparison for various treatments and sample types it was assumed that

a p-value smaller than 0.01 corresponds to significant difference between the means/average. An ANOVA table is seen in Figures 3.26 to 3.29.

Ho: Difference between treatment means is not significant
Ha: Difference between treatment means is significant

Small p value:	< 0.01	= Strong evidence against Ho
Moderate p value:	0.01 – 0.05	= Moderate evidence against Ho
Suggestive p value:	0.05 – 0.1	= Suggestive evidence against Ho
Large p value:	> 0.1	= Weak evidence against Ho

Figure 3.25 p-value & hypothesis.

For the DDGs sample type the treatment averages decreased with increasing treatment. This resulted in a decrease in particle size of 44.5% when comparing the maximum treatment average to the control mean. The t-test comparison between each treatment type and control resulted in a small p-value (<0.0001), which suggests there is strong evidence against the null hypothesis; thus there is a significant difference in particle size. The ANOVA test also resulted in a very small p-value, supporting the t-test as shown in Table 3.1. It is seen that for various treatment conditions there is significant difference between the average particle sizes.

DDGS	*Control*	*33%, 10s*	*33%, 50s*	*100%, 10s*	*100%, 50s*
Mean	473.4	433.8	375.3	360.6	267.5
St. Dev.	3.5	5.2	1.6	8.1	10.3
Var.	12.8	27.6	2.6	66.1	107.9
n	3.0	3.0	3.0	3.0	3.0
d.f.	-	8.0	8.0	8.0	8.0
t	-	23.1	74.4	57.0	95.4
p	-	< 0.0001	< 0.0001	< 0.0001	< 0.0001

Source	*D.F.*	*S.S.*	*M.S.*	*F*	*p*
Between	4	73948.6	18487.1	467.9	< 0.0001
Within	11	434.6	39.5		
Total	15	74383.2			

Table 3.1 DDGs t-test and ANOVA table.

For the solids sample type the treatment average also decreased with increasing treatment. This resulted in a decrease in particle size of 42.9% comparing the maximum treatment mean to the control mean. The t-test comparison between each treatment type and control resulted in a very small p-value (<0.0001), which suggests there is a significant difference in the average. The ANOVA test also resulted in a very small p-value, supporting the t-test as shown in Table 3.2.

Solids	*Control*	*33%, 10s*	*33%, 50s*	*100%, 10s*	*100%, 50s*
Mean	441.8	368.3	393.4	311.2	250.4
St. Dev.	8.4	8.2	15.7	9.9	9.4
Var.	71.2	68.3	247.4	99.7	88.8
n	3.0	3.0	3.0	3.0	3.0
d.f.	-	8.0	8.0	8.0	8.0
t	-	31.1	36.1	52.6	78.4
p	-	< 0.0001	< 0.0001	< 0.0001	< 0.0001

Source	*D.F.*	*S.S.*	*M.S.*	*F*	*p*
Between	4	60017.4	15004.3	143.3	< 0.0001
Within	11	1151.2	104.6		
Total	15	61168.6			

Table 3.2 Solids t-test and ANOVA table.

For the syrup sample type the treatment means also shows a decreasing trend with increasing treatment. This resulted in a decrease in particle size of 65.73% when comparing the maximum treatment mean to the control mean. The t-test comparison between each treatment type and control resulted in a very small p-value, which suggests there is a significant difference in the average. The ANOVA test also resulted in a very small p-value, supporting the t-test as shown in Table 3.3.

Syrup	*Control*	*33%, 10s*	*33%, 50s*	*100%, 10s*	*100%, 50s*
Mean	68.2	49.2	30.3	24.4	23.5
St. Dev.	5.9	2.4	4.9	3.8	0.9
Var.	35.8	6.0	24.6	14.4	0.8
n	3.0	3.0	3.0	3.0	3.0
d.f.	-	8.0	8.0	8.0	8.0
t	-	11.6	20.1	24.5	29.8
p	-	< 0.0001	< 0.0001	< 0.0001	< 0.0001

Source	*D.F.*	*S.S.*	*M.S.*	*F*	*p*
Between	4	4560.7	1140.1	76.5	< 0.0001
Within	11	163.8	14.8		
Total	15	4724.5			

Table 3.3 Syrup t-test and ANOVA table.

For the thin stillage sample type, the treatment means also shows a decreasing trend with increasing treatment. This resulted in a decrease in particle size of 74.57% when comparing the maximum treatment mean to the control mean. The t-test comparison between each treatment type and control resulted in a very small p-value, which suggests there is a significant difference in the average. The ANOVA test also resulted in a very small p-value, supporting the t-test as shown in Table 3.4.

Thin Stil.	*Control*	*33%, 10s*	*33%, 50s*	*100%, 10s*	*100%, 50s*
Mean	88.2	64.0	36.6	30.3	22.4
St. Dev.	4.0	13.3	5.9	4.8	5.6
Var.	16.1	178.4	35.5	23.8	32.0
n	3.0	3.0	3.0	3.0	3.0
d.f.	-	8.0	8.0	8.0	8.0
t	-	10.0	23.3	33.6	36.6
p	-	< 0.0001	< 0.0001	< 0.0001	< 0.0001

Source	*D.F.*	*S.S.*	*M.S.*	*F*	*p*
Between	4	8918.1	2229.5	42.8	< 0.0001
Within	11	572.1	52.0		
Total	15	9490.2			

Table 3.4 Thin stillage t-test and ANOVA table.

Additionally a two-way ANOVA was performed to test for interaction between the 2 independent variables, time and amplitude, and also compared their effect on the dependent variable, mean particle size (Table 3.5).

DDGS ANOVA Two-Factor

Source of Variation	*SS*	*df*	*MS*	*F*	*P-value*	*F crit*
Time	17195.2	1	17195.2	341.0	7.61E-08	5.3
Amplitude	24502.9	1	24502.9	486.0	1.89E-08	5.3
Interaction	912.6	1	912.6	18.1	0.002781	5.3
Within	403.3	8	50.4			
Total	43014.1	11				

Table 3.5 DDGS two-factor ANOVA.

The results of the DDGS two factor ANOVA indicated that time and amplitude were significant factors and that there is interaction between the two variables with a p-value of 0.002781 as seen in Table 3.5.

Solids ANOVA Two-Factor

Source of Variation	*SS*	*df*	*MS*	*F*	*P-value*	*F crit*
Time	6048.0	1	6048.0	47.8	0.000122	5.3
Amplitude	15987.0	1	15987.0	126.4	3.51E-06	5.3
Interaction	758.4	1	758.4	5.9	0.039	5.3
Within	1011.4	8	126.4			
Total	23804.9	11				

Table 3.6 Solids two-factor ANOVA.

The two factor ANOVA of the data from the solids indicate that time and amplitude were significant factors, and that there was moderate evidence of interaction between the two variables with a p-value of 0.039 as seen in Table 3.6.

Syrup ANOVA Two-Factor

Source of Variation	*SS*	*df*	*MS*	*F*	*P-value*	*F crit*
Time	294.0	1	294.0	25.3	0.0010	5.3
Amplitude	748.9	1	748.9	64.4	4.25E-05	5.3
Interaction	246.6	1	246.6	21.2	0.0017	5.3
Within	92.9	8	11.6			
Total	1382.4	11				

Table 3.7 Syrup two-factor ANOVA.

The two factor ANOVA of the data from the syrup, indicate that time and amplitude were significant factors, and that there was strong interaction between the two variables with a p-value of 0.0017 as seen in Table 3.7.

Thin Stillage ANOVA Two-Factor

Source of Variation	*SS*	*df*	*MS*	*F*	*P-value*	*F crit*
Time	937.2	1	937.2	13.9	0.0057	5.3
Amplitude	1714.8	1	1714.8	25.4	0.0009	5.3
Interaction	285.6	1	285.6	4.24	0.0734	5.3
Within	538.8	8	67.3			
Total	3476.5	11				

Table 3.8 Thin stillage two-factor ANOVA.

The two factor ANOVA of the data from the thin stillage indicated that time and amplitude were significant factors, and that there was suggestive evidence of interaction between the two variables with a p-value of 0.0734 as seen in Table 3.8.

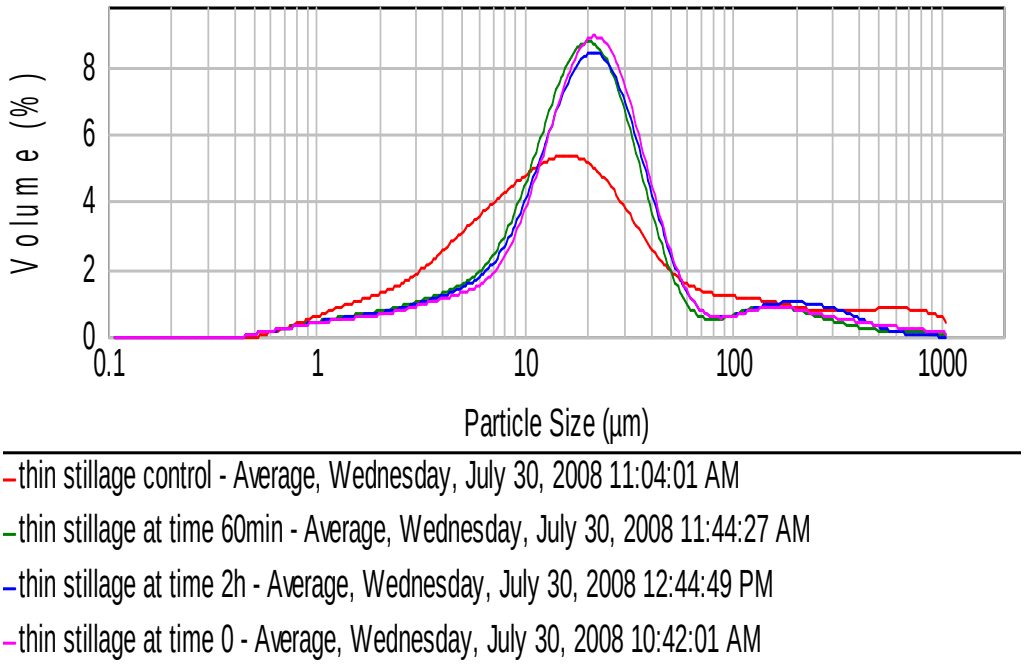

Figure 3.26 Particle size distributions with respect to time

Due to the increase in peak particle size of the treated syrup and thin stillage samples as detailed in Figures 3.23 and 3.24, it was theorized that this is due to particles agglomerating. In order to confirm this theory, thin stillage and syrup samples were characterized with the Malvern Mastersizer PDA immediately after sonication, 1 h after sonication, and 2 h after sonication comparing amplitude to time. Figure 3.26 shows particle size distribution for various time intervals after sonication for the thin stillage. It is seen that there is little difference for the various times, suggesting the agglomerates were formed during sonication.

The mean particle size by volume for the DDGs and solids for the various treatments are seen in Figure 3.27. It can be seen that with increasing treatment there is a general decrease in particle size. This is consistent with the OM and SEM images. In contrast, when a similar analysis is completed for the syrup and thin stillage samples, there is an increase in peak particle size. For these samples, the particle size was normalized as a function of dissipated energy during treatment. This increase in the peak values is shown relative to the energy input in joules as shown in Figure 3.28.

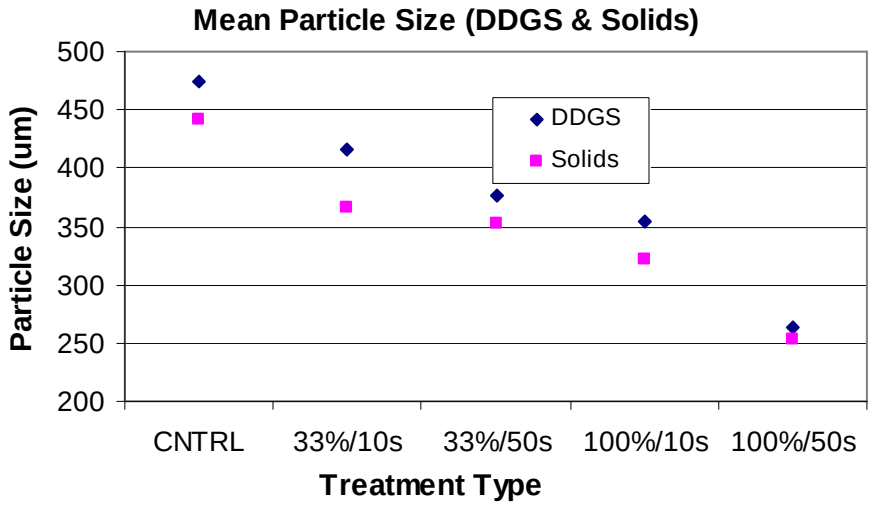

Figure 3.27 Mean particle size DDGS and solids

Again it is believed that this increase in peak particle size is due to oil droplets coalescencing and agglomerization of particles during treatment for the syrup and thin stillage samples.

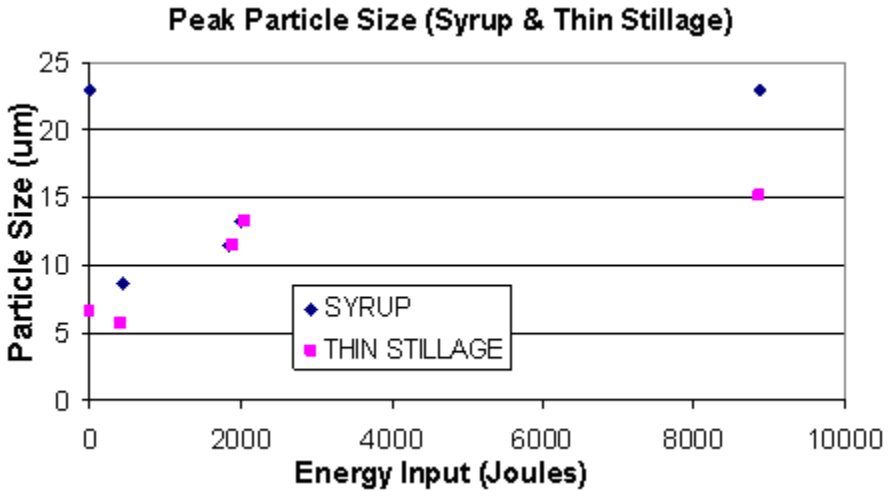

Figure 3.28 Peak particle size thin stillage and syrup

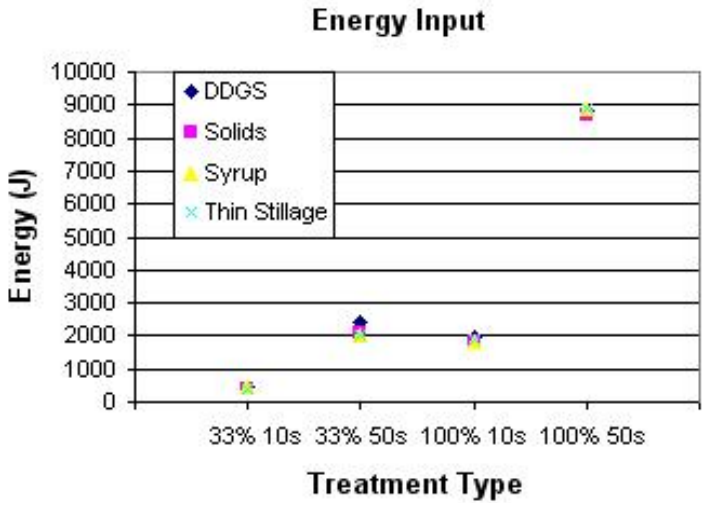

Figure 3.29 Energy input

When comparing the dissipated energy to the treatment types as shown in Figure 3.29, it is seen there is a proportional relationship between energy and time and between energy and amplitude. Both treatment types show an approximately 4x increase in power input when 40 s were added to the same amplitude setting. Figure 3.30 compares the mean particle size to energy, which also shows a decreasing trend in particle size as energy input increases.

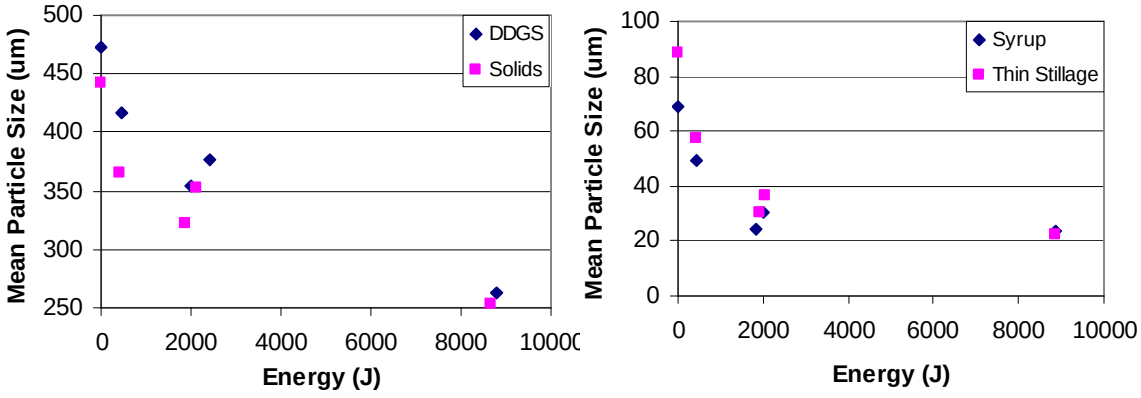

Figure 3.30 Mean particle size as a function of energy.

CHAPTER 4: CONCLUSIONS AND RECOMMENDATIONS

Analysis of the OM and SEM imaging, and PDA results show a decrease in particle size for the selected dry mill ethanol coproducts after ultrasonic treatment. It was also found that the particle size was generally inversely proportional to the amplitude and treatment time. Using the numerical data from the PDA system, the percentage of particle size decrease was calculated. It was found that there was a 44.5% decrease in the mean particle size for the DDGS, 42.9% in the solids, 65.7% in the syrup, and 74.57% in the thin stillage. It should be noted that the peak values of the thin stillage and syrup samples increase, as shown in the PDA graphs, as a shift to the right suggesting an increase in peak particle size. While misleading, this should not be confused with an overall average decrease when observing the entire curve.

The SEM images of the DDGS and solids samples showed evidence of ultrasonic destruction of the cell walls when comparing the control group to the treated samples. Cellular structure was often found to be fragmented and visually shown to have distinct porous features on the surface of the particles on the ultrasonically treated samples. Particles were also noticeably smaller in size when comparing the control to the treated samples, as this was most apparent when comparing the control to the maximum treatment.

This evidence was not present with the thin stillage and syrup samples. The SEM images of the thin stillage and syrup samples did not provide any suggestions as to have any

effect; this probably was due to the significantly initial smaller particle size. Although it was not visually as apparent, the statistical data suggests there was a difference.

In a companion paper by Wu-Haan [51], the ultrasonically pretreated samples were compared to the untreated samples for biomethane potential. In the study it was shown that ultrasonically treating the dry mill ethanol coproducts increases methane production during anaerobic digestion. The DDGs coproduct resulted in a 23% average increase in methane biogas production, and the solids showed a 10% average increase. The study further concluded that ultrasonic treatment was far more effective on the solid sample types and that it would be very beneficial if the DDGS and solid coproducts were used in methane gas production by anaerobic digestion. Because the Malvern Mastersizer particle analyzer could only measure particles smaller than 1000 µm, this research could be improved if the larger particles were also measured for the DDGS and solids samples. Future work related to this research should evaluate the potential of ultrasonics installed on an industrial scale, improving ethanol production facilities energy output by utilizing the increased biogas production from sonicated coproducts. Ultrasonics could also play a role in improved generation of value added products extracted from sonicated DDGS and solids such as oils and proteins.

REFERENCES

1 Early plant domestication. Retrieved April 4, 2008 from (http://www.athenapub.com/nwdom1.htm)

2 What is dent corn? Retrieved April 4, 2008 from (http://www.wisegeek.com/what-is-dent-corn.htm)

3 Corn. Retreieved March 20th, 2008 from (http://www.hort.purdue.edu/newcrop/Crops/Corn.html)

4 Mesoamerica image. Retrieved May 29, 2008 from (http://upload.wikimedia.org/wikipedia/commons/2/24/Region_Mesoamerica.png)

5 Corn types. Retrieved March 20th, 2008 from (http://www2.kenyon.edu/projects/farmschool/food/corntyp.htm)

6 Corn image. Retrieved June 2, 2008 from (http://en.wikipedia.org/wiki/Image:GEM_corn.jpg)

7 Specialty corns, waxy. Retrieved May 28, 2008 from (http://ohioline.osu.edu/agf-fact/0112.html)

8 What is pop corn? Retrieved May 28, 2008 from (http://www.wisegeek.com/what-is-popcorn.htm)

9 What is dent corn? Retrieved April 4, 2008 from (http://www.wisegeek.com/what-is-dent-corn.htm)

10 Yellow dent corn. Retrieved April 7, 2008 from (http://waltonfeed.com/self/corn.html)

11 Corn. Britannica Student Encyclopædia. Retrieved March 23rd, 2008 from (http://student.britannica.com/comptons/article-199219)

12 World of corn. Retrieved March 20th, 2008 from (http://www.ncga.com/worldofcorn/2007/kernel.asp)

13 Corn kernel image. Retrieved June 2, 2008 from (http://www.cerealprocess.com/images/corn-components.jpg)

14 It begins with a kernel. Retrieved March 20th, 2008 from (http://www.iowacorn.org/cornuse/cornuse_2.html)

15 Corn products. Retrieved June 3, 2008 from (www.ontariocorn.org)

16 Corn use. South Dakota Corn. Retrieved March 21st, 2008 from (http://www.sdcorn.org/cornuse/example.cfm)

17 Corn production overview. Retrieved May, 29th, 2008 from (http://www.ers.usda.gov/Briefing/Corn)

18 Trade statistics. NCGA. Retrieved March 22nd, 2008 from (http://www.ncga.com/trade/main/statistics.asp)

19 RFA industry statistics. Retrieved April 4, 2008 from (http://www.ethanolrfa.org/industry/statistics)

20 Kurt A. Rosentrater. 2007. Corn ethanol co-products - Some current constraints and potential opportunities. *International Sugar Journal* 109(1307): 685, 687-689, 691-697. CODEN: ISUJA3 ISSN: 0020-8841. AN 2007:1459876 CAPLUS

21 Kurt A. Rosentrater, Heath R. Hall, Conly L. Hansen. 2006. Anaerobic digestion potential for ethanol processing residues. Paper 066167, presented at the 2006 Annual Meeting of the American Society of Agricultural and Biological Engineers (ASABE). ASABE, St. Joseph, MI.

22 Lincoln Way Energy. Retrieved June 3, 2008 from (http://www.lincolnwayenergy.com/)

23 How ethanol is made. RFA. Retrieved March 23, 2008 from (http://www.ethanolrfa.org/resource/made)

24 Kent D. Rausch, Ronald L. Belyea. 2006. The future of coproducts from corn processing. *Applied Biochemistry and Biotechnology* 128(1): 47-86.

25 Hosein Shapouri, James Duffield, Michael S. Graboski. 1995. Estimating the net energy value of corn-ethanol. *Proceedings - Biomass Conference of the Americas: Energy, Environment, Agriculture and Industry, 2nd, Portland, OR, August 21-24, 1995,* pp. 976-985. U.S. Department of Agriculture, Office of Energy and New Uses, Washington, DC, USA.

26 David Pimentel. 2003. Ethanol fuels: Energy balance, economics, and environmental impacts are negative. *Natural Resources Research* 12(2). June.

27 Anaerobic digestion. Retrieved June 12, 2008 from (http://en.wikipedia.org/wiki/Anaerobic_digestion)

28 Kenneth S. Suslick, ed. 1988. *Ultrasound: It's Chemical, Physical and Biological Effects.* VCH Publishers, New York.

29 Ultrasound. Retrieved April 1, 2008 from (http://en.wikipedia.org/wiki/Ultrasound)

30 Ultrasound image. Retrieved April 1, 2008 from (http://www.nuh.nhs.uk/qmc/MaternityUnit-tour/images/Ultrasound.jpg)

31 Piezoelectric materials. Retrieved April 1, 2008 from (http://www.ndt-ed.org/EducationResources/CommunityCollege/Ultrasonics /EquipmentTrans/piezotransducers.htm)

32 Uchino, Kenji. "Piezoelectric Actuators and Ultrasonic Motors." 1996 Kluwer Academic Publishers. ISBN 0792398114.

33 S. Khanal, D. Grewell, S. Sung, J. Van Leeuwen. 2007. Ultrasound applications in wastewater sludge pretreatment: A review. *Critical Reviews in Environmental Science and Technology* 37(4): 277-313.

34 Brennen, Christopher. "Cavitation and Bubble Dynamics." Chapter 1, section 5. Oxford University Press, 1995. ISBN 0-19-509409-3.

35 Cavitation bubble collapse image. Retrieved June 2, 2008 from (http://www.coleparmer.com/techinfo/images/cavitationbubble_250-155.gif)

36 "Acoustic Streaming"Sci-Tech Dictionary. McGraw-Hill Dictionary of Scientific and Technical Terms. Copyright © 2003. McGraw-Hill Companies, Inc.

37 W L. Nyborg. 1997. Acoustic streaming. In: Mark F. Hamilton, David T. Blackstock. *Nonlinear Acoustics: Theory and Applications,* pp. 207-208. Academic Press.

38 Masafumi Nakagawa. 2004. Analyses of acoustic streaming generated by four ultrasonic vibrators in a vessel. *Japanese Journal of Applied Physics, Part 1: Regular Papers, Short Notes & Review Papers* 43(5B): 2847-2851.

39 Byoung-Gook Loh, Sinjae Hyun, Paul I Ro, Clement Kleinstreuer. 2002. Acoustic streaming induced by ultrasonic flexural vibrations and associated enhancement of convective heat transfer. *The Journal of the Acoustical Society of America* 111(2): 875-83. Journal code: 7503051. ISSN:0001-4966.

40 L. Clarke, A. Edwards, E. Graham. 2004. Acoustic streaming: An in vitro study. *Ultrasound in Medicine and Biology* 30(4): 559-62.

41 Crowell, Benjamin. 1998-2006 “Vibrations and Waves” Chapter 2: Resonance Pages 26-41.

42 Rossing, Thomas D., and Fletcher, Neville H., Principles of Vibration and Sound. New York, Springer-Verlag, 1995.

43 *Billah, K.;* R. Scanlan *(1991). "*Resonance, Tacoma Narrows Bridge Failure, and Undergraduate Physics Textbooks*" American Journal of Physics 59 (2): 118–124.*

44 Basics of high power ultrasonics. Retrieved April 1, 2008 from (http://www.powerultrasonics.com/content/basics-power-ultrasonics)

45 Ultrasonic tooling. Retrieved April 4, 2008 from (http://industrialultrasonics.com/horns.htm)

46 Kriss, Timothy C.; Kriss, Vesna Martich (April 1998), "History of the Operating Microscope: From Magnifying Glass to Microneurosurgery", Neurosurgery 42 (4): 899–907

47 Scanning electron microscope. Retrieved June 2, 2008 from (http://en.wikipedia.org/wiki/Scanning_electron_microscope)

48 SEM imaging. Retrieved June 2, 2008 from (http://www.purdue.edu/REM/rs/sem.htm)

49 James P M Syvitski (2007). Principles, Methods and Application of Particle Size Analysis. Cambridge University Press. ISBN-13: 9780521044615

50 Branson Ultrasonics. Retrieved April 26, 2008 from (http://www.bransonultrasonics.com)

51 W. Wu-Hann, D. Grewell, C.J. Hearn, R.T. Burns, L.B. Moody. 2008. "Characterization of Ultrasonic Pretreatment on Biogas Production Potential from Corn Ethanol By-products". Submitted to Biomass and Bioenergy on September 18, 2008 Ref. No.: JBB-D-08-00485.

52 The Zeiss Corporation. Retrieved June 3, 2008 from (http://www.zeiss.com/)

53 Hitachi America. Retrieved June 3, 2008 from (http://www.hitachi.us/)

54 Oxford Instruments. Retrieved June 3, 2008 from (www.oxford-instruments.com/)

55 Malvern Instruments. Retrieved June 3, 2008 from (www.malvern.co.uk/)

56 Samir Khanal, Melissa Montalbo, J. (Hans) van Leeuwen, Gowrishankar Srinivasan, David Grewell. 2007. Ultrasound enhanced glucose release from corn in ethanol plants, *Journal of Environmental Science and Technology* 6(6): 5-42.

57 T. Prozorov, R. Prozorov, K.S. Suslick. 2004. High velocity inter-particle collisions driven by ultrasound, *Journal of the American Chemical Society,* 126: 13890-13891.

58 David Grewell, 2008. Ultrasonic Basics. AE 590 lecture notes, pages 114-118.

59 Magnetostrictive vs Peizoelectric Transducers for Power Ultrasonic Applications. Retrieved October 19, 2008 from: (http://www.blackstone-ney.com/pdfs/T_Mag_Vs_Piezo.pdf)

60 Torija, Ma. J., N. Rozès, M. Poblet, J.M. Guillamón, and A. Mas. 2003. *Effects of fermentation temperature on the strain population of Saccharomyces cerevisiae* . International Journal of Food Microbiology. 80: 47-53.

61 Banat, I.M., P. Nigam, D. Singh, R. Merchant, and A.P. McHale. 1998. *Ethanol production at elevated temperatures and alcohol concentrations: A review; Part-I Yeast In General.* World J. Microbiol. Biotechnol. 14:809-821.

62 Erickson G.E., T.J. Klopfenstein, D.C. Adams, R.J. Rasby. 2005. General overview of feeding corn milling coproducts to beef cattle. In: Corn Processing Co-Products Manual. University of Nebraska. Lincoln, NE, USA.

VITA

September 1, 1982……..Born, Iowa City, Iowa, USA

2001……Diploma, Dubuque Senior High School
Dubuque, Iowa, USA

2006…….…….……..……B.S., Department of Industrial Technology
Iowa State University
Ames, Iowa, USA

2005…….…….……..……Manufacturing Engineering Co-Op
Mercury Marine
Fond du Lac, Wisconsin, USA

2006…….…….……..……Industrial Engineering Internship
Henderson Manufacturing
Manchester, Iowa, USA

2006 to 2008…...…….Research and Graduate Assistant
Iowa State University
Ames, Iowa, USA

2008 to present……....Operations Tech, F-22A Program
Lockheed Martin
Marietta, Georgia, USA

AWARDS

2001 Drake Relays Silver Medalist

2006 Academic Deans List

FIELDS OF STUDY

Major Field: Industrial Technology